

2012

The Role of Small Carboxylic Acids during Poly(amide) 11 Hydrolysis

John-andrew Samuel Hocker
College of William & Mary - Arts & Sciences

Follow this and additional works at: <https://scholarworks.wm.edu/etd>

 Part of the [Organic Chemistry Commons](#)

Recommended Citation

Hocker, John-andrew Samuel, "The Role of Small Carboxylic Acids during Poly(amide) 11 Hydrolysis" (2012). *Dissertations, Theses, and Masters Projects*. Paper 1539626935.
<https://dx.doi.org/doi:10.21220/s2-c6y5-x222>

This Thesis is brought to you for free and open access by the Theses, Dissertations, & Master Projects at W&M ScholarWorks. It has been accepted for inclusion in Dissertations, Theses, and Masters Projects by an authorized administrator of W&M ScholarWorks. For more information, please contact scholarworks@wm.edu.

The Role of Small Carboxylic Acids During Poly(amide) 11 Hydrolysis

John-Andrew Samuel Hocker
Greenville, VA

Bachelor of Science, The College of William and Mary, 2010

A Thesis presented to the Graduate Faculty
of the College of William and Mary in Candidacy for the Degree of
Master of Science


Department of Chemistry

The College of William and Mary
May, 2012

APPROVAL PAGE

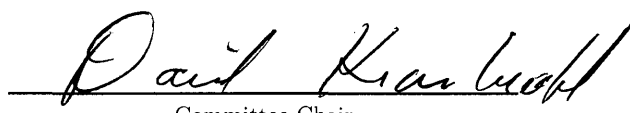
This Thesis is submitted in partial fulfillment of
the requirements for the degree of

Master of Science

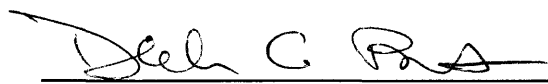


John-Andrew Samuel Hocker

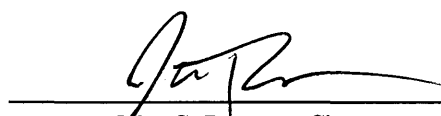
Approved by the Committee, April, 2012



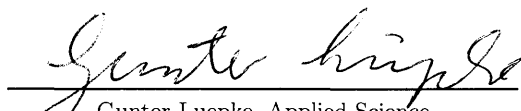
Committee Chair
David Kranbuehl, Chemistry
The College of William and Mary



Deborah C. Bebout, Chemistry
The College of William and Mary



John C. Poutsma, Chemistry
The College of William and Mary



Gunter Luepke, Applied Science
The College of William and Mary

ABSTRACT PAGE

Poly(amide)-11 (PA-11) is a member of the nylon family of polymers, and its monomer, 11-aminoundecanoic acid, is a renewable resource extracted from the castor bean. PA-11 has been used extensively as a pipe liner for non-rigid flexible pipes. The flexible pipes are employed during oil and natural gas extraction in deep water environments, allowing for transit of the resource from the wellhead to the floating platforms for processing. Hydrolysis of the PA-11 liner has been established for varying temperatures [1] [2] [3]. In 2011 Glover's PhD dissertation offered scientifically valuable information regarding small carboxylic acid ageing of PA-11 [4]. It is important to elucidate the role of the small carboxylic acids during PA-11 hydrolysis because of their presence during the extraction of crude oil and natural gas products under sub sea operating conditions. The work in this thesis presents a novel characterization of PA-11 hydrolysis kinetics as a function of varying carboxylic acids within the ageing environment. The carboxylic acids presented in this thesis are: acetic, propionic, butyric, pentanoic, naphthenic and cyclopropionic. It is shown that the kinetics of PA-11 hydrolysis per acid vary according to the acid hydrocarbon chain structure. The reason for the variance of PA-11 hydrolysis kinetics per acid is the solubility of the acid into the polymer matrix; the pH of the acid solution is shown to play no significant role.

Table of Contents

Chapter	
Acknowledgements	iii
List of Tables	iv
List of Figures	vi
1 Introduction	1
2 Instrumentation	9
2.1 Size Exclusion Chromatography-Multiple Angle Laser Light Scattering .	9
2.2 Thermogravimetric Analysis	18
3 Experimental Descriptions	21
3.1 Organic Acid Ageing Study	21
3.2 PA-11 Weight Gain Study	24
4 Results	29
4.1 Organic Acid Ageing Study	29
4.2 Weight Gain Study	42

5	Discussion	63
6	Conclusion	72
7	Future Work	73
	Bibliography	75
	Appendix	
A		77
	A.1 Procedure for pH Calculation for Known Acid Solutions	77

Acknowledgements

Professor David Kranbuehl
Dr. Arthur Jaeton Mitman Glover
Lopamudra Das
The Many Undergraduates who helped
My Employers, Colleagues, Friends, Teachers and Family.

List of Tables

Tables

1.1	Gas chromatography determined small carboxylic acid content of four production water samples. [4]	7
2.1	SEC-MALLS standard solution information for Besno P40TLOS PA-11 granules	14
2.2	Experimental $\frac{dn}{dc}$ determination: For PMMA, the $\frac{dn}{dc}$ was adjusted such that the injected mass was calculated to be $200\mu g$. For Besno P40TLOS PA-11 granules, the $\frac{dn}{dc}$ was adjusted such that the injected mass was calculated to be $175\mu g$. The $\frac{dn}{dc}$ and M_W are shown for the numbered samples; as well as the average (AVG) and standard deviation (St Dev).	15
2.3	Lab standard method for determining the volatile content of a PA-11 sample.	19
3.1	Ageing environments held at a temperature of $100^\circ C$ [5]	23
3.2	Weight Gain Study phase I, phase II, phase III methods of observation	25
3.3	Solutions used in WGS phase I, phase II and phase III.	26
3.4	TGA method used in WGS I.	27

4.1	Hydrolysis reaction constants and the solution pH's. k'_H is the hydrolysis rate constant. k'_R is the recombination rate constant. M_{We} is the equilibrium molecular weight. pH calculations are outlined in Appendix A.	34
5.1	Solubility parameters δ at standard conditions [6] [7]	67
A.1	Parameters used to calculate the pH, Appendix A	78

List of Figures

Figures

1.1	Construction of NKT Flexibles' PA-11 pipe. Layer 1 is made of steel. Layer 2 is the PA-11 liner. Layers 3 and 4 are made of steel tape. Layer 5 is an outer rubbery layer. [8]	2
1.2	11-aminoundecanoic acid, the monomer for PA-11 polymer. Note the amine on one end and the carboxylic acid on the opposing end. When an amine and a carboxylic acid undergo a condensation reaction an amide bond is formed.	3
1.3	The percent elongation at break plotted against the measured molecular weight for an array of PA-11 samples measured since 2007 in Kranbuehl Lab.	5
2.1	Schematic of the SEC-MALLS	13
2.2	SEC-MALLS example, ASTRA graphical output: Besno P40TLOS PA-11 granules with HFIP/KTFA solvent.	17
2.3	TGA report of a Besno P40TLOS granules sample. A representing water, and B representing the plasticizer	20

3.1	The molecular structures of the carboxylic acids, represented in skeletal form: (a) acetic acid (b) propionic acid (c) butyric acid (d) cyclopropionic acid (e) pentanoic acid (f) naphthenic acid	23
4.1	Hydrolysis rate constant (k'_H) plotted against the number of carbons in the acid side chain.	35
4.2	Recombination rate constant (k_R) plotted against the number of carbons in the linear acid side chain.	36
4.3	Equilibrium molecular weight (M_{We}) plotted against the number of carbons in the acid side chain.	37
4.4	Data of the linear side chain carboxylic acids; SEC-MALLS determined average molecular weight per day number aged at the 0.06% by volume concentration and 100 °C. The prediction lines determined by least squares fit to the data and structured by Equations 4.10 and 4.12 are plotted through the data points. The prediction lines are a graphical representation of the hydrolysis kinetics per ageing environment.	39
4.5	Data of the ring-containing side chain carboxylic acids; SEC-MALLS determined average molecular weight per day number aged at the 0.06% by volume concentration and 100 °C. The prediction lines determined by least squares fit to the data and structured by Equations 4.10, 4.11 and 4.12 are plotted through the data points. The prediction lines are a graphical representation of the hydrolysis kinetics per ageing environment. For comparison this graph includes the shortest (acetic) and the longest (Pentanoic) linear carboxylic acid in this study.	40

4.6	Data of the linear side chain carboxylic acids; SEC-MALLS determined average molecular weight per day number aged at the 0.36% by volume concentration and 100 °C. The prediction lines determined by least squares fit to the data and structured by Equations 4.10 and 4.12 are plotted through the data points. The prediction lines are a graphical representation of the hydrolysis kinetics per ageing environment.	41
4.7	Data of the ring-containing side chain carboxylic acid SEC-MALLS determined average molecular weight per day number aged at the 0.36% by volume concentration and 100 °C. The prediction lines determined by least squares fit to the data and structured by Equations 4.10 and 4.12 are plotted through the data points. The prediction lines are a graphical representation of the hydrolysis kinetics per ageing environment. For comparison this graph includes the shortest (acetic) and the longest (Pentanoic) linear carboxylic acid in this study.	43
4.8	WGS I: Final volatile content plotted against the number of carbons in the acid side chain per environment. This study was carried out by ageing unplasticized PA-11 beads [9] in solution at 90°C, and by using the TGA procedure displayed in Table 3.4 monitored the change in volatile content.	48
4.9	WGS I: Percent mass change of PA-11 beads [9] during ageing in acetic acid concentrations plotted against time aged. This study was carried out by ageing unplasticized PA-11 beads [9] in groups of 25 at 90°C, monitoring the change in mass using a balance.	49

4.10	WGS I: Volatile content change of a PA-11 bead [9] during ageing in acetic acid concentrations plotted against time aged. This study was carried out by ageing unplasticized PA-11 beads [9] at 90°C, and using the TGA procedure displayed in Table 3.4 monitored the change in volatile content.	50
4.11	WGS I: Percent mass change of PA-11 beads [9] during ageing in 50% by volume acid concentrations plotted against time aged. This study was carried out by ageing unplasticized PA-11 beads [9] in groups of 25 at 90°C, monitoring the change in mass using a balance.	51
4.12	WGS I: Volatile content change of a PA-11 bead [9] during ageing in 50% by volume acid concentration plotted against time aged. This study was carried out by ageing unplasticized PA-11 beads [9] at 90°C, and using the TGA procedure displayed in Table 3.4 monitored the change in volatile content.	52
4.13	WGS I: Final percent mass change of PA-11 beads [9] during ageing in 50% by volume acid concentration plotted against the number of carbons in the acid side chain per environment. This study was carried out by ageing unplasticized PA-11 beads [9] in groups of 25 at 90°C, monitoring the change in mass using a balance.	53
4.14	WGS I: Volatile content change of a PA-11 bead [9] during ageing in 50% by volume acid concentration plotted against the number of carbons in the acid side chain per environment. This study was carried out by ageing unplasticized PA-11 beads [9] in solution at 90°C, and by using the TGA procedure displayed in Table 3.4 monitored the change in volatile content.	54

4.15 WGS I: Percent mass change of PA-11 beads [9] during ageing in 75% by volume acid concentration plotted against time aged. This study was carried out by ageing unplasticized PA-11 beads [9] in groups of 25 at 90°C, monitoring the change in mass using a balance.	55
4.16 WGS I: Volatile content change of a PA-11 bead [9] during ageing in 75% by volume acid concentration plotted against time aged. This study was carried out by ageing unplasticized PA-11 beads [9] at 90°C, and using the TGA procedure displayed in Table 3.4 monitored the change in volatile content.	56
4.17 WGS I: Percent mass change of PA-11 beads [9] during ageing at low acid concentrations plotted against time aged. This study was carried out by ageing unplasticized PA-11 beads [9] in groups of 25 at 90°C, monitoring the change in mass using a balance.	57
4.18 WGS I: Volatile content change of a PA-11 bead [9] during ageing at low acid concentrations plotted against time aged. This study was carried out by ageing unplasticized PA-11 beads [9] at 90°C, and using the thermogravimetric analysis procedure displayed in Table 3.4 monitoring the change in volatile content.	58
4.19 WGS II: Percent mass change of a PA-11 bead [9], during ageing in low acetic acid by volume concentrations, plotted against time aged. This study was carried out by ageing a single unplasticized PA-11 bead [9] immersed in 2mL of stock solution at 100°C, monitoring the change in mass using a balance.	59

4.20	WGS II: Percent mass change of a PA-11 bead [9], during ageing in low butyric acid by volume concentrations, plotted against time aged. This study was carried out by ageing a single unplasticized PA-11 bead in 2mL of stock solution at 100°C, monitoring the change in mass using a balance.	60
4.21	WGS III: Volatile content change in PA-11 beads [9] during ageing in acetic and butyric acid at low concentrations plotted against time aged. This study was carried out by ageing 3 grams of unplasticized PA-11 beads [9] in 10mL of stock solution at 100°C, and using the Thermogravimetric analysis procedure outlined in Table 2.3 monitored the change in volatile content.	62
5.1	Calculated acid solution pH plotted against the number of carbons in the acid side chain.	69
5.2	The mechanism for acid catalyzed hydrolysis of an amide bond. [10] . .	70
5.3	The reciprocal of the square of the difference between the solubility parameters of PA-11 and the linear side chain acids plotted against the number of carbons in the linear acid side chain.	71

Chapter 1

Introduction

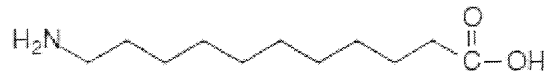
According to Rex Tillerson, CEO of Exxon-Mobil Corporation: “Deepwater production, which did not exist prior to 1989, today makes up 15 percent of all non-OPEC production. By 2030, it will grow to nearly 20 percent. Along with Brazil and West Africa, the Gulf of Mexico is one of the most important deepwater provinces in the world. In 2008, there was more oil and gas discovered in deep water than in onshore and shallow water combined. For the sake of our energy security, and the economic growth and jobs that depend on the production of these supplies, we simply cannot afford to turn our backs on this resource.”[11]

In attempts to satisfy the population’s dependence upon crude oil, techniques to accomplish deep water drilling have been engineered. A vital part of those techniques is the composition and characteristics of the pipeline, or riser. The risers’ construction, monitoring and maintenance are technologically demanding. The typical riser consists of multiple layers, as can be seen in Figure 1.1. This figure shows a cross section of the typical NKT riser as would be seen near a flange. The inner layer (1) is flexible “z-locked” steel that protects against abrasion during maintenance and against collapse when pumping is ceased under the high pressures of deep sea. The inner layer (1) is surrounded by a polymer layer (2), typically poly(amide)-11 (PA-11). It is the polymer layer that contains the crude oil during extraction. The outer layers (3,4) are typically



Figures 1.1: Construction of NKT Flexibles' PA-11 pipe. Layer 1 is made of steel. Layer 2 is the PA-11 liner. Layers 3 and 4 are made of steel tape. Layer 5 is an outer rubbery layer. [8]

steel tape wound around the flexible inner liner. The steel tape layers are designed to contain the 200+ psi pressures as well as reinforce the polymer liner against radial and axial stress. The outer layer (5) is made of rubber and guards against abrasion [8]. NKT flexible risers are operating in the Gulf of Mexico, South America, West Africa, the Mediterranean, North Sea, the Far East and Australia. [12] NKT risers often employ Poly(amide) 11 (PA-11) as the polymer liner, the second layer of the riser.



11-aminoundecanoic acid

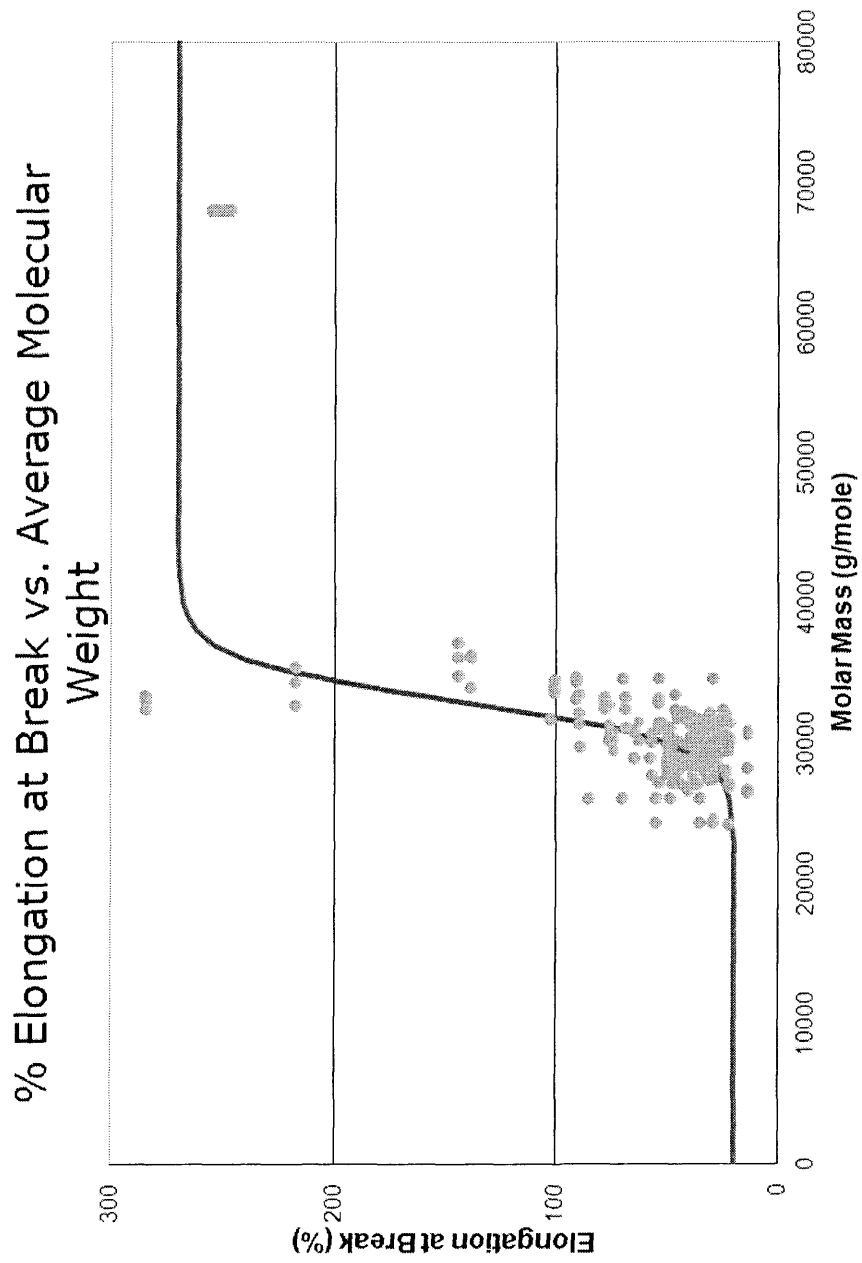
Figures 1.2: 11-aminoundecanoic acid, the monomer for PA-11 polymer. Note the amine on one end and the carboxylic acid on the opposing end. When an amine and a carboxylic acid undergo a condensation reaction an amide bond is formed.

PA-11 is a polymer matrix made through a condensation reaction (equation 4.2) of 11-aminoundecanoic acid (Figure 1.2). In a condensation reaction water is removed such that an amide group and a carboxylic acid group come together to form an amide bond. The opposing reaction is termed amide hydrolysis, where water is added to the amide bond, breaking the bond. The balance between condensation rate and hydrolysis rate of amide bonds is considered to be an equilibrium reaction. An equilibrium reaction is where a steady state concentration of formed bonds is maintained for a given set of reaction kinetics. The number of monomers present in a given polymer chain determines the molecular weight of the polymer chain. A polymer matrix is a large array of independently Gaussian coiled polymer chains, consisting of repeated monomer units, entangled with one another. The average molecular weight of a given polymer sample is the average molecular weight of each of the polymer chains in the

polymer sample. Certain aspects concerning the state of the polymer matrix can be observed by monitoring the average molecular weight of a polymer matrix.

The average molecular weight can be used to predict the mechanical properties of a given polymer matrix. Each polymer molecule has a molecular weight that is a function of the number of monomers that are in the polymer molecular chain. In a polymer matrix that consists of a very high average molecular weight, the polymer molecules in the matrix have a high relative entanglement and the mechanical properties show comparatively higher toughness (the area under a stress strain curve). Conversely, if in a polymer array the average molecular weight is low, then there is low entanglement of the polymer chains and therefore the toughness is comparatively lower. Toughness is often correlated to the percent elongation, or strain percent, with a higher percent elongation being proportional to higher toughness and vice versa for a polymer matrix type. In Figure 1.3 the percent elongation at break is plotted against the average molecular weight for an array of PA-11 samples measured since 2007 in Kranbuehl Lab. A noticeable trend is seen where the percent elongation drops drastically with the decreasing molecular weight, this is called the ductile-brittle transition. With the toughness being a function of how well the molecular chains of the polymer matrix are entangled with each other, and entanglement a function of the average molecular weight, it can be seen how the molecular weight is used as an indicator for changes in mechanical properties of a given polymer matrix [13].

For the application of PA-11 to the riser pipe construction, if the polymer's total strain percent is at or below 50% it is considered to be brittle and no longer fit for use. According to Figure 1.3 this occurs when the average molecular weight is near $30,000 \frac{g}{mole}$. If the average molecular weight is at or below the ductile-brittle transition ($\sim 30,000 \frac{g}{mole}$) then the polymer may show a brittle strain percent, which could lead to catastrophe if left unattended. However, if the PA-11 is in an environment where the



Figures 1.3: The percent elongation at break plotted against the measured molecular weight for an array of PA-11 samples measured since 2007 in Kranbuehl Lab.

equilibrium average molecular weight is higher than $\sim 30,000 \frac{g}{mole}$, not approaching the ductile-brittle transition, the PA-11 layer in the riser is understood to have an indefinite lifetime.

Midst normal operating conditions, the pumping of crude oil from the beneath the sea floor allows the sea water to fill the underground oil reservoir. Over time, as more oil is pumped from the reservoir, sea water becomes a larger component of the crude product. The sea water that gets into the riser during the pumping of crude oil is called production water. The chemical components of production water have been studied using gas chromatography, and the relative concentrations of small carboxylic acids for four samples of production water are listed in Table 1.1. Due to their presence amid the extraction of crude oil and natural gas products in sub sea operating conditions, it is important to elucidate the role of the small carboxylic acids during PA-11 hydrolysis kinetics.

Funding has been available for the study of PA-11 hydrolysis kinetics and the long term effectiveness of PA-11 in offshore sub sea operating conditions. In 2002, Meyer et al. characterized a kinetic model for PA-11 ageing in a pH 7 water environment [1]. Then in 2003 Verdu et al. offered a kinetic model for acid catalysed hydrolysis of PA-11 [14]. Eight years later, in 2011, Glover's dissertation offered scientifically valuable information regarding small carboxylic acid ageing of PA-11 [4]. Each of these studies characterizes the resulting hydrolysis degradation kinetics per environment by monitoring the changes in the average molecular weight for PA-11 polymer samples.

The work in this thesis presents a novel characterization of PA-11 hydrolysis kinetics in the presence of varying carboxylic acid environments. Two experimental motifs are presented in this thesis: a study of organic carboxylic acid catalysed hydrolysis in PA-11 and a PA-11 weight gain study. In the organic acid ageing study, it is hypothesized that the kinetics of PA-11 hydrolysis per acid molecule concentration will vary according to

Production Water Sample	Acid Name	Acid Concentration (ppm)
RIS305A	acetic	1043
	3-propionic	80
	butyric	13
	pentanoic	3
RIS305C	acetic	708
	3-propionic	56
	butyric	3
	pentanoic	2
RIS305A	acetic	1364
	3-propionic	51
	butyric	0
	pentanoic	2
RIS305A	acetic	992
	3-propionic	25
	butyric	3
	pentanoic	12

Tables 1.1: Gas chromatography determined small carboxylic acid content of four production water samples. [4]

the acid side chain structure. In the weight gain study it is hypothesized that higher concentrations and longer linear side chain acids will show preferential solubility in the PA-11 matrix.

Chapter 2

Instrumentation

2.1 Size Exclusion Chromatography-Multiple Angle Laser Light Scattering

2.1.1 Introduction

Multiple Angle Laser Light Scattering (MALLS) is a primary method of determining the weight average molar mass (M_W) of a polymer sample. A primary method uses a direct measurement to characterize the M_W of a sample. Size Exclusion Chromatography (SEC) performs fractionation of a dissolved sample according to relative chain size. Pairing the SEC with the MALLS (SEC-MALLS) fractionates the dissolved polymer sample and determines the molecular weight of each resulting fraction. Using the molecular weights of the fractions, the M_W of a sample was calculated.

2.1.2 Theory

SEC involves passing a sample through a medium in which there are pores of a similar size and shape as the hydrodynamic volume of the sample. SEC is used to fractionate a dissolved polymer sample based on the hydrodynamic volume of the polymer chain. Fractionation is attained by forcing a dissolved polymer sample through a High Performance Liquid Chromatography (HPLC) system. The HPLC system contains a series of in-line SEC columns. The SEC columns are packed using small polymer pack-

ing beads. The beads must be composed of a substance that is chemically inert with respect to the solvent and the polymer sample. The design of the beads includes a perforation of channels.

The SEC will fractionate the polymer sample based on the size of the perforations in the beads. The polymer chains with a larger hydrodynamic volume do not fit into smaller channels, and thus pass between the packing beads. However, the chains with smaller hydrodynamic volume fit into the perforations and readily pass through the channels. As the smaller chains pass through many channels and the larger chains pass through few, there is a difference in path length through the column. Larger chains have a shorter path length than smaller chains. The polymer chains with larger hydrodynamic volumes will elute from the column series first. The channels through the packing beads are required to be capable of effectively interacting with the range of polymer chain sizes present in the polymer samples.

The system used in this thesis employed multiple in-line SEC columns: HFIP-LG, HFIP-805, and HFIP-803 from Shodex. The packing beads were composed of a polystyrene-divinyl benzene copolymer. The different model numbers indicate different pore designs in the beads. The HFIP-LG column performs negligible separation and is present to capture destructive impurities before they reach the more expensive analytical columns. The HFIP-805 follows the HFIP-LG column, containing packing beads that separate at a $4 \times 10^6 g/mole$ of polystyrene exclusion limit. The final column that the dissolved polymer is forced through, having packing beads with the smallest pore size, is the HFIP-803 column. The HFIP-803 column separates at a $7 \times 10^4 g/mole$ of polystyrene exclusion limit. [15]

Once the dissolved polymer sample is fractionated by SEC, the Multiple-Angle Laser Light Scattering (MALLS) technique was used to characterize the molecular weight of the sample fractions. The MALLS technique measures Rayleigh light scattering when

a laser passes through a dissolved polymer solution. A Zimm plot can be used to calculate the molecular weights of the polymer solution fractions. Zimm plots use an array of concentrations to extrapolate to a zero angle and zero concentration. On the other hand, a Debye plot assumes very dilute output of the SEC is an approximation to zero concentration, with a zero angle extrapolation. In this thesis a Debye plot was used to characterize the M_W of the polymer samples. Therefore, at any given time, to relate the scattering angle and intensity to the radius of gyration and average molecular weight of a polymer sample having passed through our HPLC system, we can consider equations 2.1 and 2.2:

$$\frac{Kc}{R_\theta} \approx \frac{1}{\overline{M}_W [1 - \frac{16\pi^2}{3\lambda^2} \langle r_g^2 \rangle \sin^2 \frac{\theta}{2}]} \quad (2.1)$$

where c is concentration $\frac{g}{cm^3}$, R_θ excess Rayleigh ratio (intensity of scattered light to intensity of incident light at angle θ), \overline{M}_W - weight-averaged molar mass, λ - wavelength of light scattered, $\langle r_g^2 \rangle$ - mean square radius of gyration, θ - detection angle of scattered light and K is an optical constant defined by equation 2.2:

$$K = \frac{4\pi^2 n_0^2}{N_A \lambda_0^4} \left(\frac{dn}{dc} \right)^2 \quad (2.2)$$

where n_0 - pure solvent refractive index, N_A - Avogadro's number, and $\frac{dn}{dc}$ - refractive index increment of polymer in the solvent. The refractive index increment is defined to be the change in refractive index per unit concentration change of solute in solution.

For light scattering detection we use a Wyatt miniDAWN light scattering detector. The miniDAWN has a $\lambda = 690\text{nm}$ and three detection angles $\theta = 45^\circ, 90^\circ, 135^\circ$. With the miniDAWN gathering the necessary scattering information for M_W characterization of a dissolved polymer sample, to satisfy 2.1 the concentration c data for the various fractions is also needed. [16] [17]

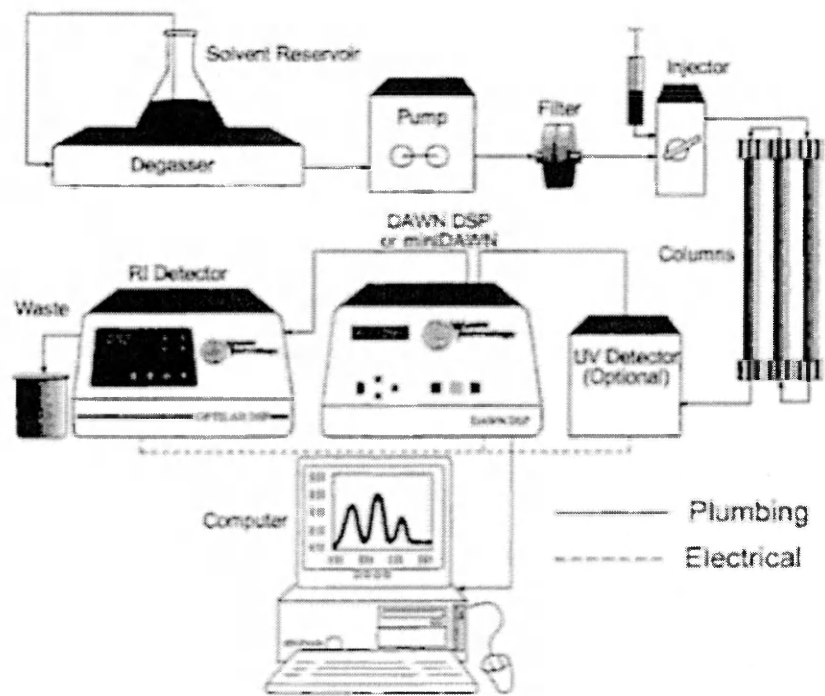
Typically the concentration is characterized either by an Ultra Violet (UV) absorbance detector or a Refractive Index (RI) detector. In this case, the system uses

a Wyatt Optilab 803 dynamic RI detector in-line with the HPLC columns and the miniDAWN. Using an experimentally determined $\frac{dn}{dc}$ of 0.263, the signal from the Optilab 803 detection cell was used to determine c for the fractions of SEC eluent.

To pressurize the SEC-MALLS system, in-line 1/16" outside diameter stainless steel tubing was paired with a Waters 515 HPLC pump. The Waters 515 HPLC pump has a dual-plunger design; and due to the minute differences between the two plungers, pressure fluctuations of 5-10 psi occurred. Pressure fluctuations in the line would produce noise in the detected signals. Increasing the total pressure of the system made pressure fluctuations produced by the two plungers less pronounced. An undetermined length of 0.005" inner diameter stainless steel tubing was added post-detector to increase the total pressure of the system: total pressure 540 ± 40 psi.

Fluctuations in the system's overall precision also occurred from periodic clogging of the frit and temperature changes in the lab HVAC system (Heating Ventillation and Air Conditioning). The frit was a $2\mu m$ $\frac{1}{8}$ " outer diameter filter [18] through which each injection of dissolved polymer sample initially passed through and was used to filter the injection of larger debris that might cause damage to the subsequent columns. When the frit became congested, the system pressure increased, and the frit was immediately replaced. Temperature fluctuations of the HVAC system affected the RI detection precision and were minimized by the installation of a temperature reservoir. The temperature of the reservoir would fluctuate between 20°C and 23°C over 16 hour periods. The reservoir temperature fluctuation was accounted for each morning when the RI detector baseline was established.

The solvent used to dissolve the polymer samples was 1,1,1,3,3,3-hexafluoroisopropan-2-ol (HFIP) doped with $7\frac{mg}{mL}$ Potassium Tri-Fluoroacetate (KTFA) salt. The solvent was degassed in the pump reservoir via constant Helium sparge under atmospheric pressure.



Figures 2.1: Schematic of the SEC-MALLS

Property	Value	Units
Mass of HFIP+KTFA	8.066 ± 0.0001	<i>g</i>
Volume of HFIP+KTFA	5.041 ± 0.0001	<i>mL</i>
Mass of Polymer Sample	10.1 ± 0.1	<i>mg</i>
Volatile Content	12.7 ± 0.5	%
Corrected Polymer Mass	8.81 ± 0.04	<i>mg</i>
Corrected Solution Concentration	1.75 ± 0.01	$\frac{mg}{mL}$
Injected Mass	175 ± 1	μg
Independently Verified M_W	39000 ± 2000	$\frac{g}{mole}$

Tables 2.1: SEC-MALLS standard solution information for Besno P40TLOS PA-11 granules

2.1.3 Sample Preparation

To maintain reliably accurate and precise results, two polymer standards were established for the work done in this thesis. The two standards were: BESNO P40TLOS PA-11 granules and a Polymethyl Methacrylate (PMMA) standard produced by *Polymer Laboratories*. A standard polymer solution was injected daily before PA-11 sample solutions were injected, serving to verify that the system was working properly. The BESNO PA-11 standard has an independently verified M_W of 39000 ± 2000 g/mole while the PMMA standard has a commercially marketed 28900 ± 1000 g/mole. The difference in uncertainty for each of the two samples could be explained by the homogeneity of the individual standards. The polymer sample heterogeneity could have been amplified due to the very small portions of polymer used for dissolving the 2mg/mL sample solutions. Table 2.1 offers solution information representative of both standards as well as any sample solution used in this thesis.

Table 2.2 shows the observed averages and standard deviations for the M_W 's and $\frac{dn}{dc}$'s of the two standards: Besno PA-11 and PMMA. It has been established that for different polymer systems there is a unique $\frac{dn}{dc}$ associated that must be determined prior to calculating molar mass results [17]. To find the exact $\frac{dn}{dc}$ for a polymer sample,

a thermogravimetric analysis (TGA) of the sample is performed. The method of the TGA is designed such that the volatile content present in the polymer is quantified. With the volatile content known, an exact concentration of the polymer solution is calculated. Given the exact concentration of the injected solution, multiple runs would be conducted and the average $\frac{dn}{dc}$ necessary to calculate the exact polymer mass injected would be ascertained [19]. Using the experimentally determined $\frac{dn}{dc}$ value, the M_W of the polymer sample is calculated, an example of this is seen in Table 2.2 where $\frac{dn}{dc}$'s were determined for multiple solutions of each standard.

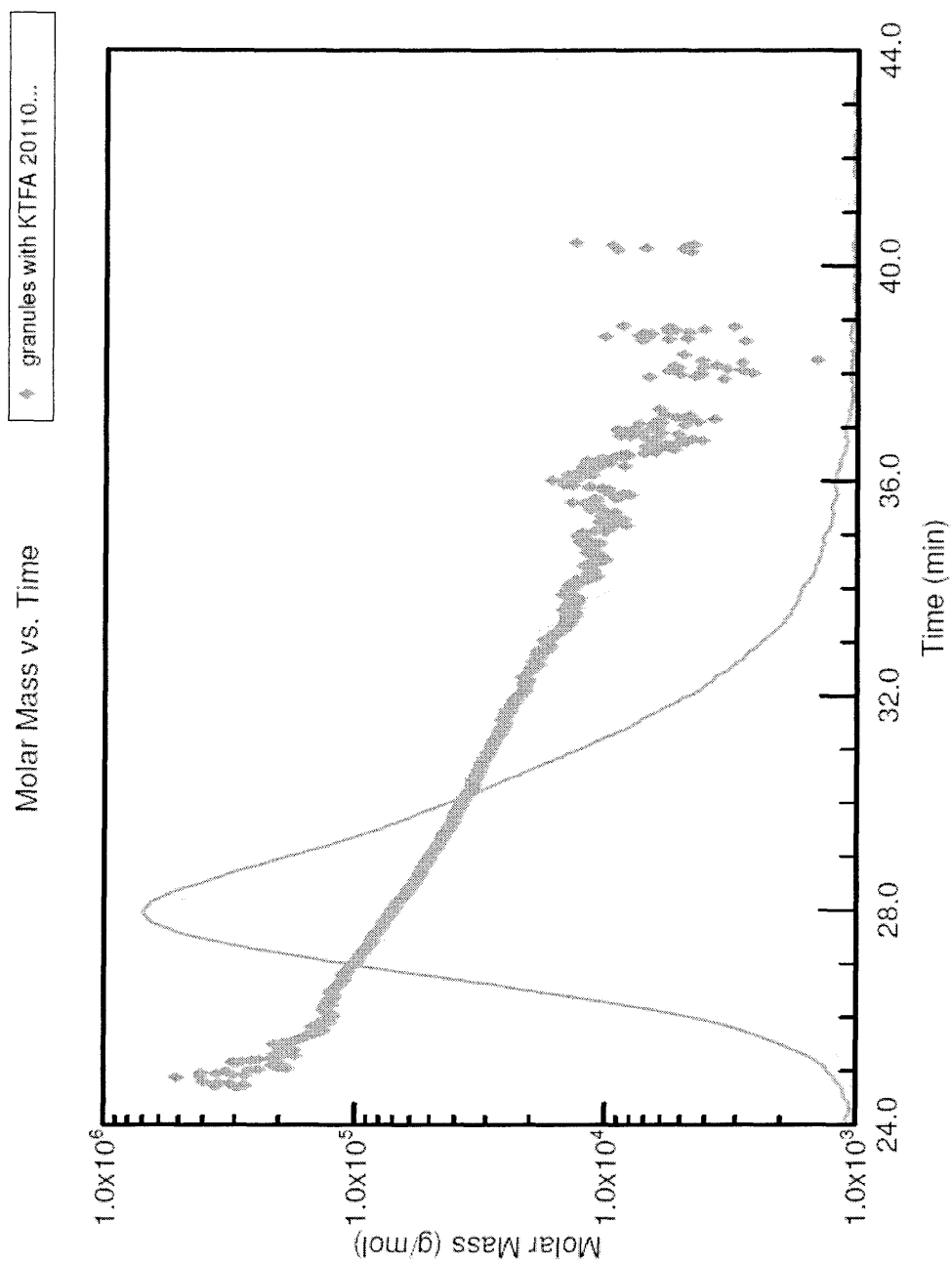
	PMMA		Besno PA-11	
	$\frac{dn}{dc}$	M_W	$\frac{dn}{dc}$	M_W
1	0.1999	30200	0.3333	42300
2	0.2067	29680	0.333	40270
3	0.2124	27630	0.344	37150
4	0.2013	28600	0.3432	42900
5	0.2075	28780	0.326	40700
6	0.2093	29910	0.3882	37860
7	0.2053	29880	0.379	38710
AVG	0.2061	29240	0.3495	39980
St Dev	0.0044	861	0.0242	2184

Tables 2.2: Experimental $\frac{dn}{dc}$ determination: For PMMA, the $\frac{dn}{dc}$ was adjusted such that the injected mass was calculated to be $200\mu g$. For Besno P40TLOS PA-11 granules, the $\frac{dn}{dc}$ was adjusted such that the injected mass was calculated to be $175\mu g$. The $\frac{dn}{dc}$ and M_W are shown for the numbered samples; as well as the average (AVG) and standard deviation (St Dev).

2.1.4 Output

All polymer sample solutions were mixed at 2 mg/mL. For data collection, $100\mu L$ of a sample solution volume was injected. Once the injected sample passed through all detectors, Wyatt Technologies' ASTRA software recorded the output in a computer data file. The data file contained a chromatogram from the three light scattering angles

from the miniDAWN as well as concentration information from the RI detector. Once the sample had eluted into the waste vessel baselines for each detector in the system were established using the ASTRA program. With the baselines established the data from each detector was combined and the peak area selected. ASTRA used the user defined $\frac{dn}{dc}$, baselines and peak selection to generate a report of the analyzed data. Figure 2.2 shows a graphical report generated by the ASTRA software.



Figures 2.2: SEC-MALLS example, ASTRA graphical output: Besno P40TLOS PA-11 granules with HFIP/KTFA solvent.

2.2 Thermogravimetric Analysis

2.2.1 Theory

Thermogravimetric Analysis(TGA) is a technique that monitors the mass change of a material as a function of temperature. While a TGA has many applications, for the work in this thesis the TGA was applied to the determination of volatile content for various polymer samples. With volatile content for the polymer samples, the true polymer solution concentration was determined.

The instrument used for the experiments presented here was a model Q500 from TA Instruments. The model Q500 features a programmable furnace with a high temperature of 1000.0°C, mass determination to the nearest microgram and a programmable gas flow sample chamber. The sample chamber is set up so that nitrogen gas is constantly purging the environment of oxygen, so as to prevent oxidation while heating the sample. If the polymer samples were to be exposed to oxygen while in the melted state, a reduction in mass would ensue because of CO₂ and H₂O evolution. When the mass of the sample is reduced due to the formation and subsequent evaporation of CO₂ and H₂O, an overestimation of the volatile content results. For overestimated volatile content the calculated mass, and consequently the determined $\frac{dn}{dc}$, inherit a systematic error.

2.2.2 Sample Preparation

The preparation of sample consists of using a stainless steel razor blade to cut slices of the polymer no thicker than *1mm*. A pyrolysis-cleaned platinum pan was tared on the instrument, and the thin slices are placed on that pan. The pan and the sample are then loaded in the instrument. Table 2.3 shows the method used to determine the volatile content of a polyamide sample. The first step ensures that oxidation will not

Step	Action
1	Select N ₂ as the purge gas
2	Ramp at 10°C per minute to 105°C
3	Isothermal for 45 minutes
4	Ramp at 10°C per minute to 240°C
5	Isothermal for 120 minutes

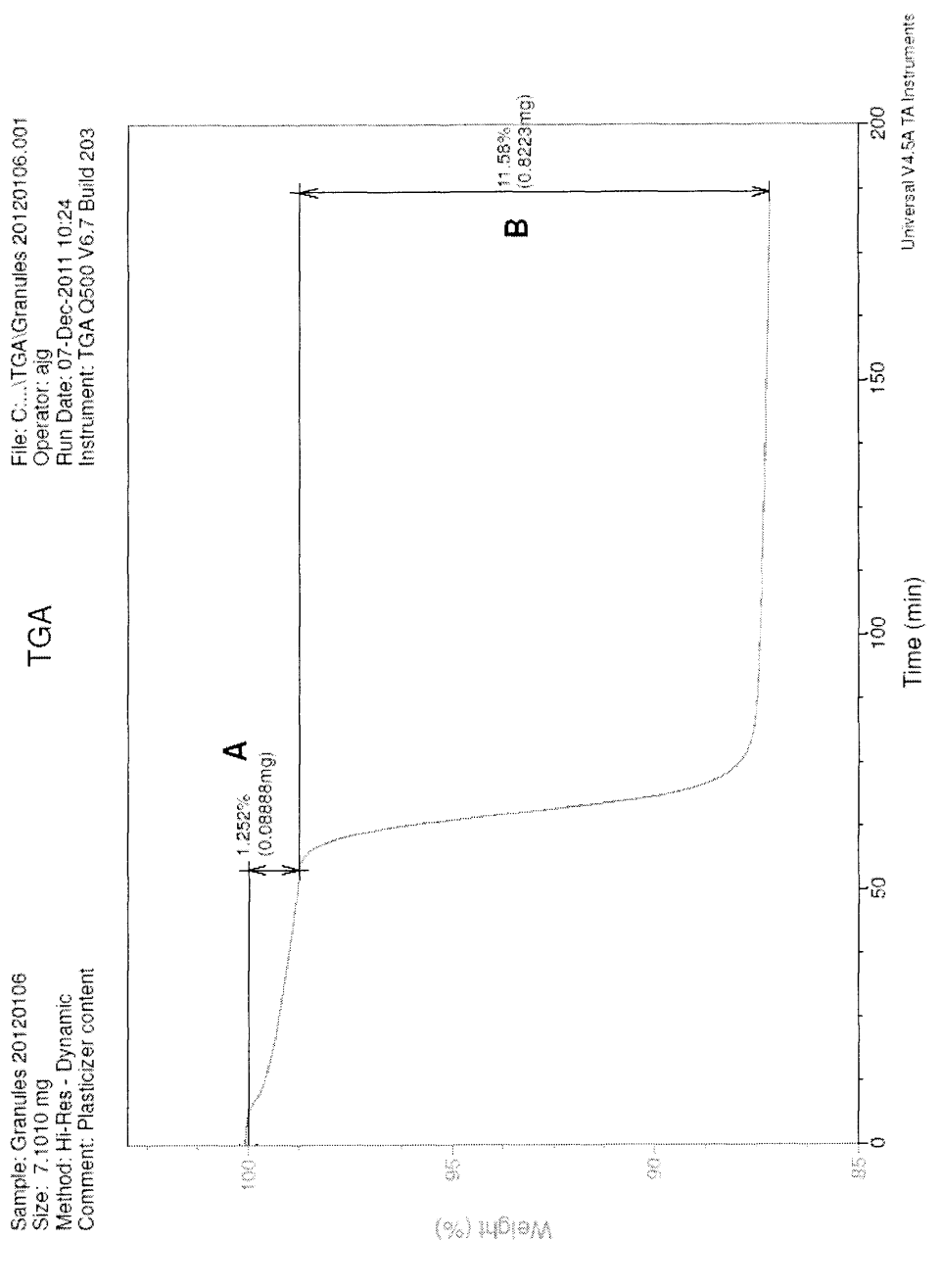
Tables 2.3: Lab standard method for determining the volatile content of a PA-11 sample.

interfere with the results. The second and third are meant to evaporate water. The fourth and fifth steps evaporate the remaining volatile content, which was typically taken to be the plasticizer content.

2.2.3 Output Example

The data files that the TGA produced were paired with the TA Universal Analysis software. TA Universal Analysis software displayed the data file as a plot of percent mass loss vs. time. The user then used Universal Analysis to analyze and annotate the plot with the desired information. Figure 2.3 shows a typical PA-11 volatile content thermogravimetric analysis. Figure 2.3 shows that the typical sample had 1.3% water and 11.58% plasticizer content. This is consistent with the published total volatile content of $12.7\% \pm 0.2$. [20]

Knowing that this particular instrument model (Q500 from TA Instruments) precisely records both the temperature and the mass of the sample during the experiment, it can be inferred that the sources of error were limited to the sampling. In general PA-11 samples display heterogeneity, so for representative sampling, large samples required repeated experiments across optimally spaced intervals.



Figures 2.3: TGA report of a Besno P40TLOS granules sample. **A** representing water, and **B** representing the plasticizer

Chapter 3

Experimental Descriptions

3.1 Organic Acid Ageing Study

3.1.1 Theory

In 2002 Meyer et al. [1] characterized and presented a model of PA-11 hydrolysis in a pH 7 water environment. In 2003 Verdu et al. [14] published a characterization and model of hydrolytic ageing of PA-11 in the presence of CO₂. The organic acid ageing experimental design was devised to further extend such isolated studies pertaining to the understanding of PA-11 degradation in deep sea oil field environments. The hypothesis of this organic acid ageing study is that the equilibrium kinetics of PA-11 hydrolysis per acid concentration will vary according to the acid side chain structure.

Meyer's 2002 publication offers insight into PA-11 hydrolysis and a useful mathematical model, but does not engage the catalytic effects of other chemicals that may be present during PA-11 applications. The 2003 publication presents the effects of CO₂ on PA-11 hydrolysis. This work established that carbonic acid, a weak acid, can influence the equilibrium of PA-11 hydrolysis by further catalysing the process towards higher conversions via amine scavenging. Their organic acid ageing study was designed to characterize either the amine scavenging or catalytic effects of carboxylic acids during PA-11 hydrolysis. The hypothesis of the organic acid ageing study presented in this thesis is that the equilibrium kinetics of PA-11 hydrolysis per acid concentration will

vary according to the acid side chain structure.

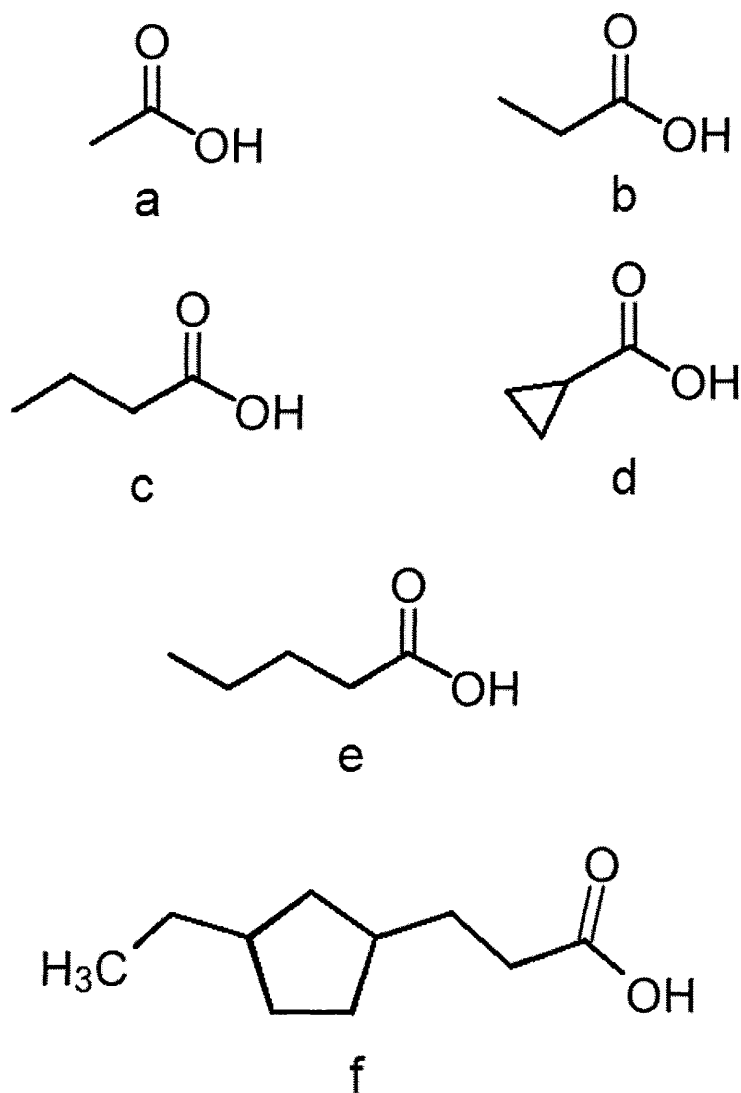
3.1.2 Implementation

The ageing environment was created by inserting twelve 1cm^3 PA-11 coupons into single ACE no. 8648 heavy walled glass pressure tubes. A specific organic acid solution was poured into each tube. The volume of the acid solution submerged the polymer coupons. The volume of the acid solution added was at least twice the volume of the polymer coupons. To maintain an internal standard, both solvents, mineral oil and water, were present in each tube at equivalent volumes. The polymer coupons were placed in the acid containing solution within the tube. The solutions within the prepared pressure tubes were sparged with argon gas, to remove oxygen, sealed and then placed in a 100°C oven for ageing.

All polymer sample coupons in this study were cut from a single large sample piece of commercial NKT PA-11. This manufactured flexible pipe liner PA-11 sample was chosen for its wide use throughout the world. The ageing coupons, cubical with a 1cm^3 dimension, were cut from a localized area of NKT pipeliner PA-11 polymer.

The polymer coupons were subjected to an array of solvent-temperature-specific environments, outlined in Table 3.1. As can be seen in Table 3.1, the following combination of parameters were used in this study; there were six small carboxylic acids: acetic, butyric, cyclopropionic, naphthenic, propionic and pentanoic; two concentrations by volume for each acid: 0.36%, 0.06%; two solvents used: deionized water, mineral oil; all with the temperature held at a constant 100°C . The molecular structure of each acid used is shown in Figure 3.1.

For all acid solutions, a series of dilutions was used to achieve the desired concentrations. For the 0.36% and 0.06% by volume solutions, a starting stock solution was first prepared. The starting solution was a 3.6% by volume solution, made by adding



Figures 3.1: The molecular structures of the carboxylic acids, represented in skeletal form: (a) acetic acid (b) propionic acid (c) butyric acid (d) cyclopropionic acid (e) pentanoic acid (f) naphthenic acid

Linear Carbons	Acid Name	Solvent			Acid Manufacturer	pK _a
		Deionized Water	Mineral Oil	% Purity		
1	Acetic	x		Glacial	Fisher	4.75
2	Propionic	x		99.5	Aldrich	4.87
3	Butyric	x		99+	Aldrich	4.81
4	Pentanoic		x	99	Aldrich	4.82
	Cyclopropionic	x		95	Aldrich	
	Napthenic		x	N/A	Fluka	

Tables 3.1: Ageing environments held at a temperature of 100°C [5]

3.6mL acid to 96.4mL solvent. The 0.36% solution was prepared using 10mL of the stock solution and 90mL of solvent. The 0.06% solution was prepared using 4.17mL of stock solution and 90mL of solvent. Table 3.1 displays information describing the starting materials used for the stock solutions.

For Tubes with mineral oil/acid solutions an aliquot of $\sim 5\text{cm}^3$ deionized water was placed at the bottom of the tube. For tubes with water/acid solutions an aliquot of $\sim 5\text{cm}^3$ mineral oil was layered atop the acid solution. All the tubes with liquid and polymer present were then bubbled with argon gas for 30 minutes to purge the oxygen out of solution. The oxygen was removed to a concentration below 0.05 mg/L, as measured by an Oakton DO110 series oxygen meter [21]. The tubes were then sealed and subsequently submerged in an ethylene glycol bath. The ethylene glycol bath with the tubes submerged was then aged in the oven set at a temperature of 100 °C. The coupons underwent accelerated ageing for 189 days. The time-scale of 189 days was chosen such that sufficient time was allowed for the PA-11 samples to show evidence of an equilibrium molecular weight.

Coupons were extracted from the pressure tube environments intermittently during the 189 day ageing period. When the coupons were sampled the solution and solvent layers were replenished, argon sparged, and with an air-tight seal the pressure tube was returned to the oven. With each sampling, the coupon's average molecular weight was

characterized via SEC-MALLS measurements.

3.2 PA-11 Weight Gain Study

3.2.1 Theory

The PA-11 weight gain study was devised to monitor the overall mass change a polymer sample undergoes during environment specific ageing processes. In this thesis the hypothesis of the weight gain study was that the longer side chain carboxylic acids show preferential solubility in PA-11.

3.2.2 Implementation

The weight gain study consisted of multiple phases. The polymer chosen for the various phases of the weight gain study was an unplasticized commercial PA-11 bead [9]. The PA-11 beads were not of a uniform shape or size. As can be seen in Table 3.2 three weight gain study phases were carried out, each employing a different method of observation. Phase one monitored the changing state of the PA-11 bead through two different methods of observation: a grouped 25 bead mass, as measured on a balance and a single bead examined for volatile content, as measured via thermogravimetric analysis. Phase two monitored the changing mass of a single bead in 2mL of aqueous acid solution using a digital scale. Phase three monitored the changing volatile content of the sample beads using thermogravimetric analysis. Table 3.3 contains the different acid solutions used to create each of the ageing environments studied in the three phases.

Phase I Part one: 25 bead grouped mass The beads were taken in clusters of 25, and wrapped in a steel cloth packet. The packet of 25 was inserted into a single ACE no. 8648 heavy walled glass pressure tube. The packet was then submerged by

Weight Gain Study Phase	Mass 25 Beads	Mass Single Bead	Thermogravimetric Analysis	Ageing Temperature
I	x		x	90 °C
II		x		100 °C
III			x	100 °C

Tables 3.2: Weight Gain Study phase I, phase II, phase III methods of observation

Linear Carbons	Acid Name	Acid Concentration					
		0.06%	0.36%	2%	10%	50%	75%
1	Acetic	I,II,III	I,II,III	II	I,II	I	I
2	Propionic					I	I
3	Butyric	II,III	II,III			I	I
4	Pentanoic	I	I			I	I
	Cyclopropionic					I	I

Tables 3.3: Solutions used in WGS phase I, phase II and phase III.

one of the acid solutions used in phase I as listed in Table 3.3. The same solvent, polymer and pressure tube design as was used in the organic acid ageing study was used in this study; both solvents were present in each tube. A 30 minute argon sparge was used to remove all oxygen before the tubes were sealed and placed in the 90°C oven.

To collect data, the 25 bead packet was removed from the pressure tube. Once removed, the 25 beads were individually dried by use of a KimWipe. The mass of the dried 25 bead cluster was then measured with a balance having an accuracy of $\pm 1^{-4}$ g. The cluster of beads was then returned to the stainless steel cloth envelope, and the envelope was returned to the pressure tube where fresh acid solution and an equivalent aliquot of the alternate solvent was added before the tube underwent a 30 minute argon sparge, air-tight seal and a return to the 90°C oven.

Part two: single bead volatile content Ten beads were placed in a separate steel cloth packet and paired into the same conditions as the beads in phase I-part one weight gain study.

To collect data, a single bead was taken from the count of ten, and the volatile content was measured via thermogravimetric analysis. The remaining count of beads was subsequently re-inserted into the ageing environment with the paired group of 25 from phase I-part one weight gain study. The thermogravimetric analysis algorithm performed on the single bead samples is listed in Table 3.4.

Step	Action
1	Select N ₂ as the purge gas
2	Ramp at 1°C per minute to 180°C

Tables 3.4: TGA method used in WGS I.

Phase II

Single bead mass change A single uniquely shaped bead was placed in the bottom of each ACE no. 8648 heavy walled glass pressure tube. The bead was then submerged by one of the phase II associated acid solutions as listed in Table 3.3. Each tube contained a single bead submerged in $2mL$ of acid solution. With the bead and the solution placed in the bottom of the pressure tube, the tube was air-tight sealed and placed in the $100^{\circ}C$ oven for ageing.

To collect data for this experiment the pressure tube ensemble was first cooled to room temperature. The single unique bead was extracted, dried with a KimWipe and was measured using a balance having an accuracy of $\pm 1^{-4}g$. The pressure tube was rinsed and dried, cleaned of solution residue. The PA-11 sample bead was returned to the cleaned pressure tube, the aliquot of $2mL$ solution was replenished and the ensemble was sealed for further ageing in the $100^{\circ}C$ oven.

Phase III

Volatile content change of PA-11 bead at low concentrations A three gram mass of the PA-11 sample was placed in the bottom of each ACE no. 8648 heavy walled glass pressure tube. The three grams of beads were submerged using $10mL$ of a phase III acid solution as listed in Table 3.3. Once the beads and the solution were inside the pressure tube, the tube was given an air-tight seal and replaced in the $100^{\circ}C$ oven for further ageing.

To collect data for this experiment the pressure tube was removed from the oven and equilibrated to room temperature. Then, a single bead was extracted and patted dry of aqueous acid solution. Each bead extracted was tested via the TGA standard plasticizer routine (Table 2.3). Maintaining the same solution and collection of beads, the tube was resealed and placed back into the $100^{\circ}C$ oven for further ageing.

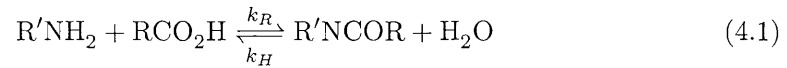
Chapter 4

Results

4.1 Organic Acid Ageing Study

4.1.1 PA-11 Hydrolysis

Equation 4.1 represents the amide hydrolysis chemical equilibrium reaction.



Modelling PA-11 Hydrolysis The following is the mathematical model of polyamide hydrolysis kinetics with no acid present. The following mathematical treatment assumes no previous ageing of the sample.

$$-\frac{d[\text{R}'\text{NH}_2]}{dt} = -\frac{d[\text{RCO}_2\text{H}]}{dt} = k_R[\text{R}'\text{NH}_2][\text{RCO}_2\text{H}] - k_H[\text{R}'\text{NCOR}][\text{H}_2\text{O}] \quad (4.2)$$

$[\text{R}'\text{NH}_2]$ is the concentration of amine end groups and $[\text{RCO}_2\text{H}]$ is the concentration of carboxylic end groups, increasing concentration of either within a PA-11 matrix is indicative of amide bond hydrolysis. k_R the recombination rate constant (a condensation reaction) of hydrolysed amide bonds. k_H the hydrolysis rate constant as it effects amide bonds within the PA-11 matrix. $[\text{R}'\text{NCOR}]$ the concentration of amide bonds and $[\text{H}_2\text{O}]$ is the concentration of water within the PA-11 matrix at any given time.

The concentration of H_2O can be incorporated into the k_H term by assuming a large and constant concentration of H_2O . The k_H term is then represented by a pseudo first

order rate constant k'_H . Since each broken amide bond would theoretically yield one amine and one carboxyl group, we will assume stoichiometric formation; represented in equation 4.3

$$-\frac{d[\text{R}'\text{NH}_2]}{dt} = -\frac{[\text{RCO}_2\text{H}]}{dt} = k_R[\text{RCO}_2\text{H}]^2 - k'_H[\text{R}'\text{NCOR}] \quad (4.3)$$

Equation 4.3 can be equivalently expressed by equation 4.4.

$$\frac{dx}{dt} = k'_H(a_0 - x) - k_R x^2 \quad (4.4)$$

Where x is the amine or acid concentration at time t , and a_0 is the initial average number of amide bonds in the polymer sample. Equation 4.5 is derived from the steady state approximation

$$k_R = \frac{k'_H(a_0 - x_e)}{x_e^2} \quad (4.5)$$

where x_e represents the equilibrium product concentration. Substitution of equation 4.5 into equation 4.4 yields equation 4.6. [22, page 21]

$$\frac{dx}{dt} = k'_H(a_0 - x) - \frac{k'_H(a_0 - x_e)}{x_e^2} x^2 \quad (4.6)$$

Separation of variables and integration of equation 4.6 gives equation 4.7. [22]

$$\frac{x_e}{(2a_0 - x_e)} \ln \left(\frac{a_0 x_e + x(a_0 - x_e)}{a_0(x_e - x)} \right) = k'_H t \quad (4.7)$$

Given equations 4.8 and 4.9

$$x = a_0 - a \quad (4.8)$$

$$x_e = a_0 - a_e \quad (4.9)$$

substituted into equation 4.7, equation 4.10 results. [22]

$$\left(\frac{a_0 - a_e}{a_0 + a_e}\right) \ln \left(\frac{a_0^2 - a_e a}{a_0(a - a_e)}\right) = k'_H t \quad (4.10)$$

Rearrangement and substitution of equation 4.5 yields equation 4.11

$$k_R = \frac{k'_H a_e}{(a_0 - a_e)^2} \quad (4.11)$$

For the final calculations equation 4.12 is required. [4] Where $M_n = \frac{M_W}{2}$ is assumed for a condensation polymer (PA-11 is a condensation polymer) and 183.29 is the molecular weight of the monomer, equation 4.12 is derived, and the number of amide bonds is effectively defined in terms of the average molecular weight.

$$a = \left(\frac{M_W}{2 \times 183.29}\right) - 1 \quad (4.12)$$

4.1.2 Data

Using equations 4.10, 4.11 and 4.12 and the M_W data obtained for the organic acid ageing study, a non-linear least squares fit to the organic acid ageing study was performed. Thus, for each acid ageing environment a unique set of kinetic parameters was obtained. The three parameters were: hydrolysis rate constant (k'_H), recombination rate constant (k_R), and equilibrium molecular weight (M_{We}). The parameter values determined in this thesis can be observed in Table 4.1. Also included in Table 4.1 is the calculated pH of each acid solution; the details of which can be found in Appendix A.

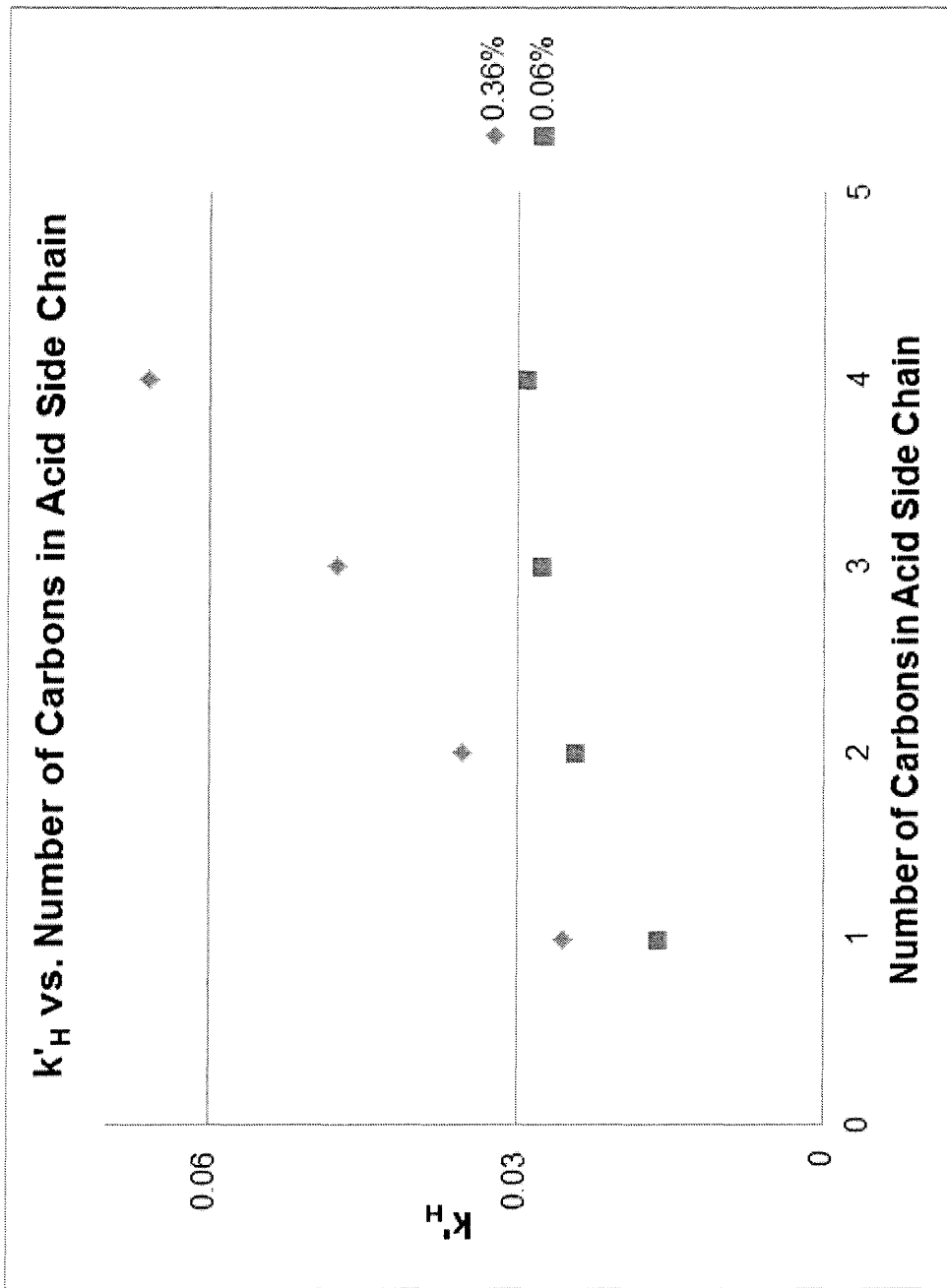
These parameters were used in equations 4.10 and 4.12 to generate $M_W(\frac{g}{mole})$ curves for the ageing of PA-11 in the different acid environments. The ageing curves are plotted alongside the associated data in Figures 4.6, 4.7, 4.4 and 4.5.

The four plots used to compare the data are separated by the two concentrations of the stock solutions and the molecular structure of the individual acids. Figures 4.4 and 4.5 display data taken at the 0.06% concentration. Figures 4.6 and 4.7 show the data at the 0.36% concentration. Figures 4.4 and 4.6 offer a comparison of the different acids based on the length of their linear side chains. Figures 4.5 and 4.7 include the ring containing acids, as they compare to the smallest and the largest linear side chain acids. Deionized water was the standard control used in this study, and is displayed on each graph. The molecular structures of the acids used in this study can be seen in Figure 3.1.

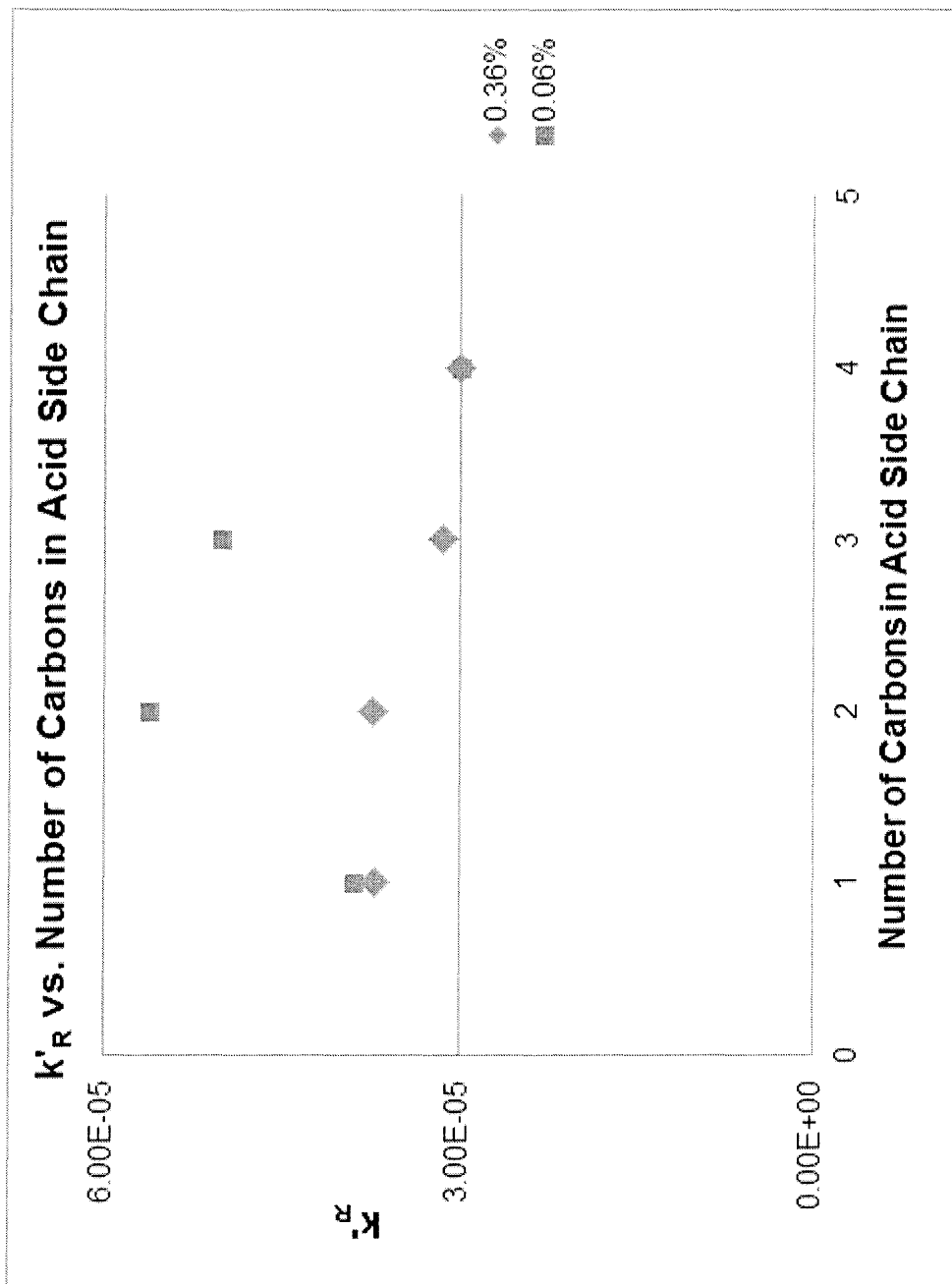
Table 4.1 shows that the hydrolysis rate constant increases from DI water to acetic, butyric, propionic, butyric, naphthenic, pentanoic, to cyclopropionic for both concentrations. The recombination rate constant does not show a monotonic trend for the various acid in the two concentrations. Corresponding to the trend in the hydrolysis rate constant, the equilibrium molecular weight is shown to decrease per acid in the same order, with the higher concentration producing the lower equilibrium molecular weights. Lastly, a trend in the calculated pH is seen for the four linear side chain carboxylic acids, increasing with the length of the chain, and decreasing with the higher concentration. Each of these trends is seen clearly in Figures 4.1, 4.2, 4.3, and 5.1.

Linear Carbons	Solution	k'_H ($\times 10^{-2}$)	k_R ($\times 10^{-5}$)	M_{We} [$\frac{g}{mole}$]	Calculated pH
	DI Water	1.28	4.08	30350	7
0.06%					
1	Acetic	1.61	3.87	26260	4.64
2	Propionic	2.42	5.61	25290	4.76
3	Butyric	2.76	5.00	21880	4.80
4	Pentanoic	2.91	2.98	15440	4.85
	Napthenic	2.88	4.76	21090	5.10
	Cyclopropionic	3.51	1.58	8320	4.76
0.36%					
1	Acetic	2.55	3.72	19490	4.18
2	Propionic	3.53	3.74	15420	4.30
3	Butyric	4.76	3.14	10830	4.32
4	Pentanoic	6.59	3.00	8040	4.37
	Napthenic	4.74	4.44	14490	4.60
	Cyclopropionic	10.51	2.20	4440	4.30

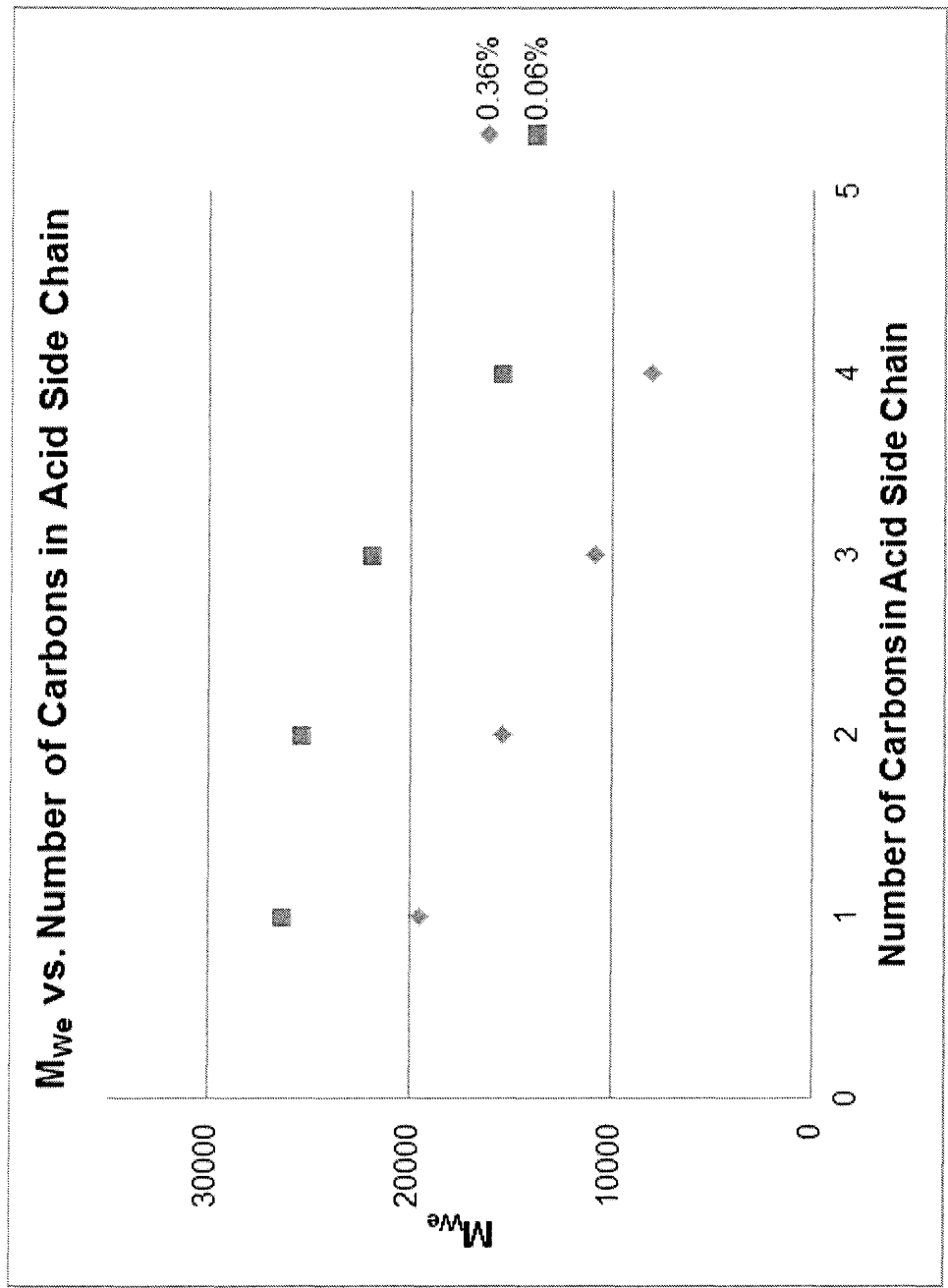
Tables 4.1: Hydrolysis reaction constants and the solution pH's. k'_H is the hydrolysis rate constant. k'_R is the recombination rate constant. M_{We} is the equilibrium molecular weight. pH calculations are outlined in Appendix A.



Figures 4.1: Hydrolysis rate constant (k'_H) plotted against the number of carbons in the acid side chain.



Figures 4.2: Recombination rate constant (k_R) plotted against the number of carbons in the linear acid side chain.



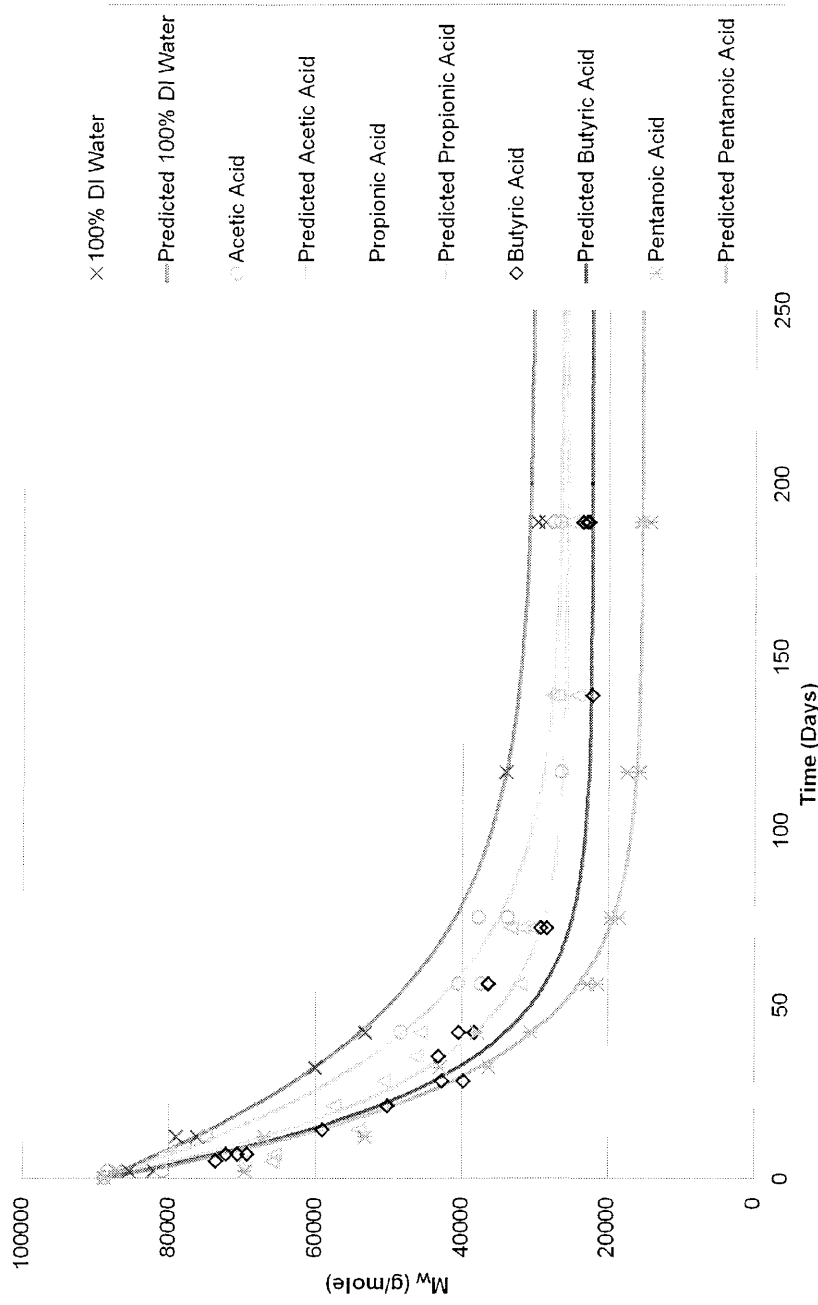
Figures 4.3: Equilibrium molecular weight (M_{We}) plotted against the number of carbons in the acid side chain.

Figure 4.4 shows the data of the linear side chain carboxylic acids; SEC-MALLS determined average molecular weight per day aged at the 0.06% by volume concentration and at 100 °C. The prediction lines, determined by a least squares fit to the data and structured by Equations 4.10 and 4.12, are plotted through the data points. The prediction lines are a graphical representation of the hydrolysis kinetics per ageing environment. The linear side chain carboxylic acid data shows hydrolysis kinetics that produce a significantly lower equilibrium average molecular weight per acid than that of deionized water. Ranging from acetic, propionic, butyric and pentanoic the data does show a wide spread, due to the low concentration. The differences between the hydrolysis kinetics of the different acids are less pronounced. The associated kinetics can be reviewed in Table 4.1.

Figure 4.5 shows the data of the ring-containing side chain carboxylic acids; SEC-MALLS determined average molecular weight per day number aged at the 0.06% by volume concentration and 100 °C. The prediction lines, determined by a least squares fit to the data and structured by Equations 4.10 and 4.12, are plotted through the data points. The prediction lines are a graphical representation of the hydrolysis kinetics per ageing environment. The ring containing carboxylic acid data shows hydrolysis kinetics that produce a significantly lower equilibrium average molecular weight per acid than that of acetic acid and deionized water. The naphthenic acid has a higher equilibrium molecular weight than pentanoic acid, whereas cyclopropionic acid exhibits a lower equilibrium molecular weight. These trends are well defined, but not well modelled to the linear side chain carboxylic acid environments. The associated kinetics can be reviewed in Table 4.1.

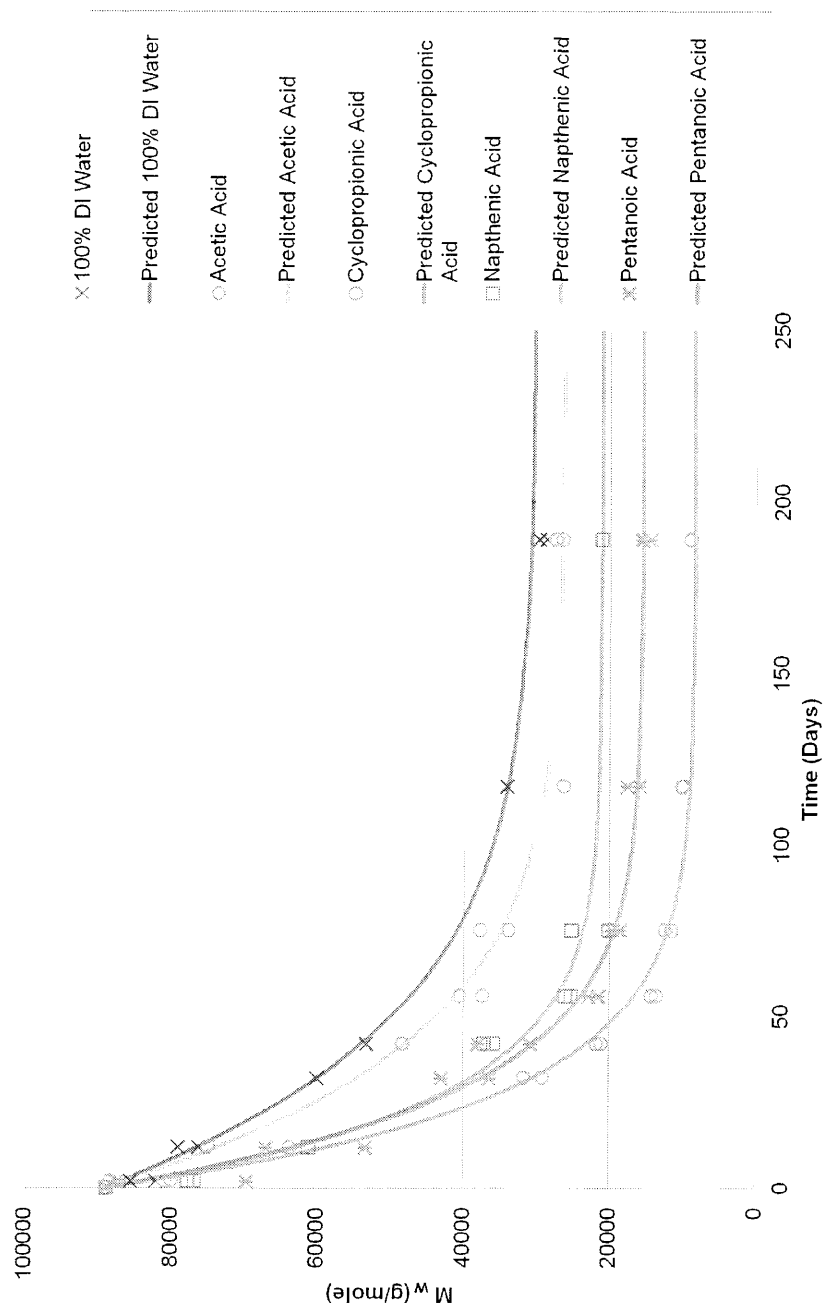
Figure 4.6 shows the data of the linear side chain carboxylic acids; SEC-MALLS determined average molecular weight per day number aged at the 0.36% by volume concentration and 100 °C. The prediction lines, determined by a least squares fit to the

MALLS MW vs. Time
Fresh Commercial PA-11 (NKT) Aged in 0.06% by Volume Acid Solutions @ 100C
Linear Acid Side Chain Comparison

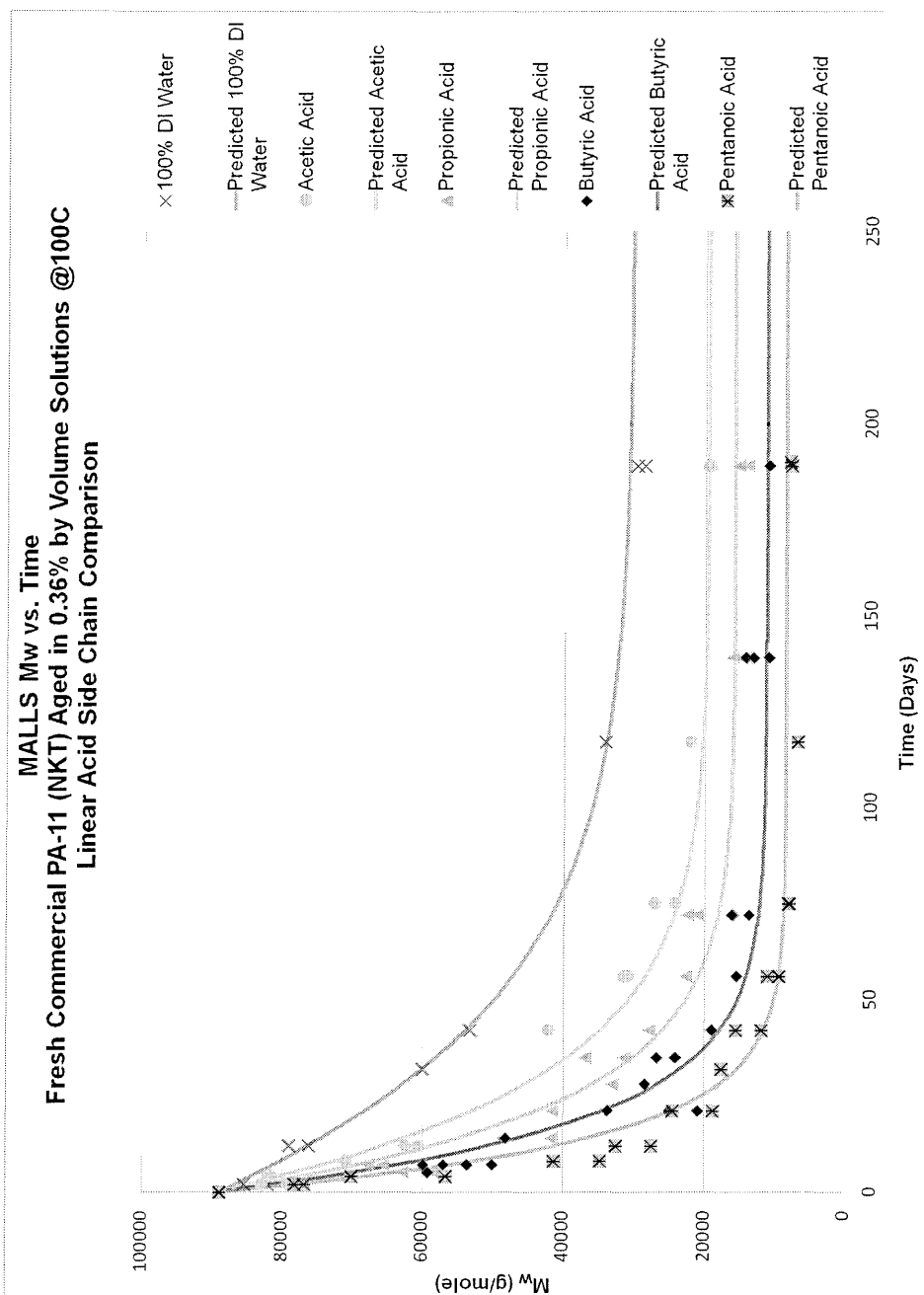


Figures 4.4: Data of the linear side chain carboxylic acids; SEC-MALLS determined average molecular weight per day number aged at the 0.06% by volume concentration and 100 °C. The prediction lines determined by least squares fit to the data and structured by Equations 4.10 and 4.12 are plotted through the data points. The prediction lines are a graphical representation of the hydrolysis kinetics per ageing environment.

MALLS Mw vs. Time
 Fresh Commercial PA-11 (NKT) Aged in 0.06% by Volume Solutions @ 100C
 Ring Containing Acid Side Chain Comparison



Figures 4.5: Data of the ring-containing side chain carboxylic acids; SEC-MALLS determined average molecular weight per day number aged at the 0.06% by volume concentration and 100 °C. The prediction lines determined by least squares fit to the data and structured by Equations 4.10, 4.11 and 4.12 are plotted through the data points. The prediction lines are a graphical representation of the hydrolysis kinetics per ageing environment. For comparison this graph includes the shortest (acetic) and the longest (Pentanoic) linear carboxylic acid in this study.



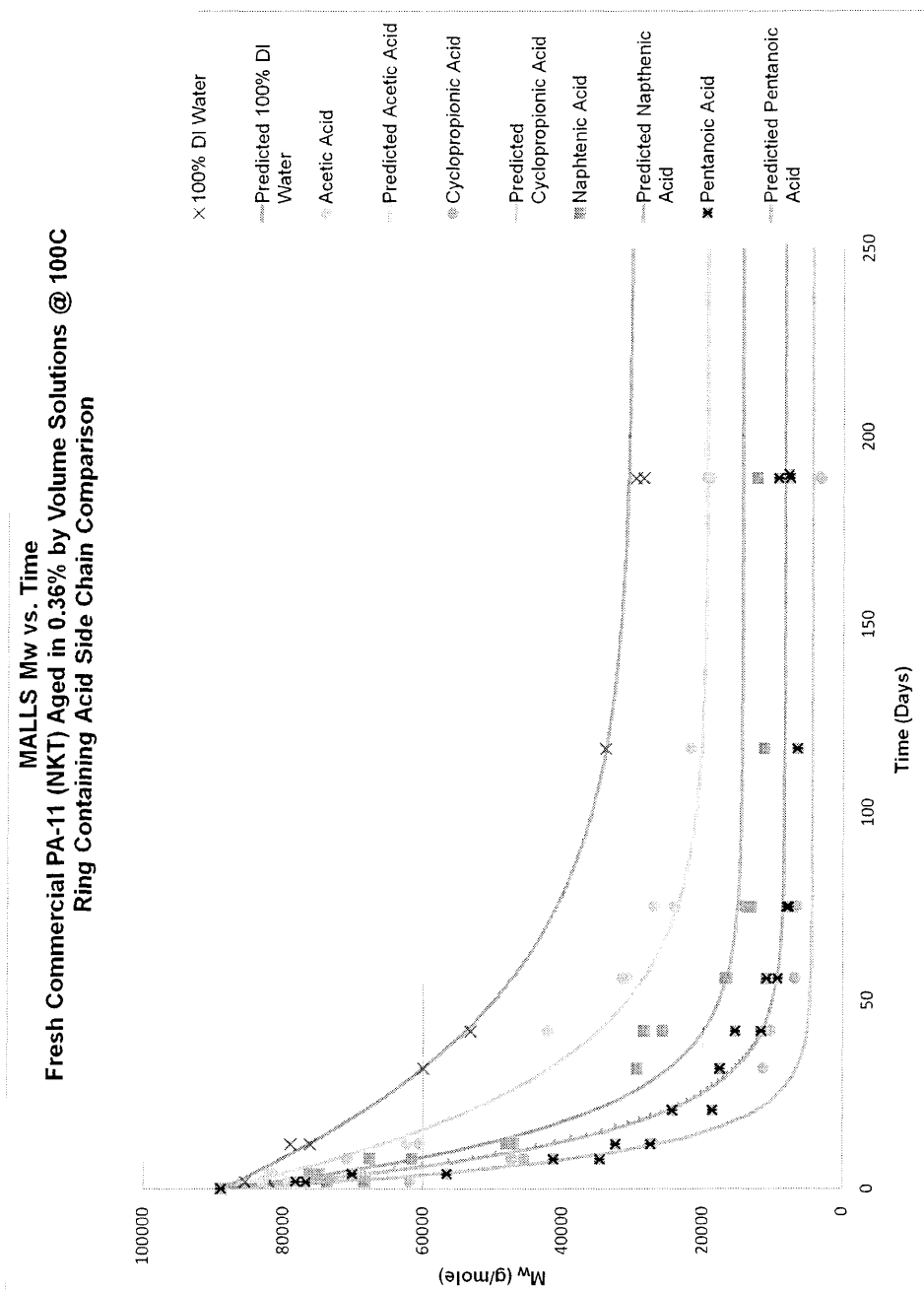
Figures 4.6: Data of the linear side chain carboxylic acids; SEC-MALLS determined average molecular weight per day number aged at the 0.36% by volume concentration and 100 °C. The prediction lines determined by least squares fit to the data and structured by Equations 4.10 and 4.12 are plotted through the data points. The prediction lines are a graphical representation of the hydrolysis kinetics per ageing environment.

data and structured by Equations 4.10 and 4.12, are plotted through the data points. The prediction lines are a graphical representation of the hydrolysis kinetics per ageing environment. The data shows hydrolysis kinetics that produce a significantly lower equilibrium average molecular weight per acid than that of the lower concentration, 0.06% by volume. The differences in the hydrolysis kinetics are significantly more pronounced at the higher concentration 0.36% by volume than the lower concentration. The associated kinetics can be reviewed in Table 4.1.

Figure 4.7 shows the data of the ring-containing side chain carboxylic acids; SEC-MALLS determined average molecular weight per day number aged at the 0.36% by volume concentration and 100 °C. The prediction lines, determined by a least squares fit to the data and structured by Equations 4.10 and 4.12, are plotted through the data points. The prediction lines are a graphical representation of the hydrolysis kinetics per ageing environment. The ring containing carboxylic acid data shows hydrolysis kinetics that produce a significantly lower equilibrium average molecular weight per acid than that of acetic acid, deionized water and the lower concentration ring containing carboxylic acids. The naphthenic acid has a higher equilibrium molecular weight than pentanoic acid, whereas cyclopropionic acid exhibits a lower equilibrium molecular weight. These trends are well defined, but not well modelled to the linear side chain carboxylic acid environments. The associated kinetics can be reviewed in Table 4.1.

4.2 Weight Gain Study

The weight gain study went through three phases: The first phase was developed to broadly characterize the PA-11 mass and volatile content changes according to the specific acid present in the ageing environment, and observe how well we could characterize this using the tools at hand. The higher concentrations were used to broadly characterize the mass and volatile changes of the PA-11 matrix when aged in the vary-



Figures 4.7: Data of the ring-containing side chain carboxylic acid SEC-MALLS determined average molecular weight per day number aged at the 0.36% by volume concentration and 100 °C. The prediction lines determined by least squares fit to the data and structured by Equations 4.10 and 4.12 are plotted through the data points. The prediction lines are a graphical representation of the hydrolysis kinetics per ageing environment. For comparison this graph includes the shortest (acetic) and the longest (Pentanoic) linear carboxylic acid in this study.

ing acid solutions. The low concentrations were examined for both acetic and pentanoic because of the linear chain acids, each showed the lowest and the highest hydrolysis rate constants. Napthenic acid was omitted from the weight gain study due to its variability in shape, size and pKa. (Napthenic acid was included in the organic acid ageing study due to its presence in crude oil). Cyclopropionic acid was included because it portrayed the most increased hydrolysis rate constant in the organic acid ageing study. Each of the linear side chain acids were included because of their comparative structures.

The second phase was derived in an attempt to more precisely examine what percent mass changes occur when ageing at the low concentrations. The third phase was created to more precisely examine what volatile content changes occur in the PA-11 matrix while ageing at the low concentrations. Butyric acid and acetic acid were chosen for phase II and phase III for two reasons: firstly time management and secondly because butyric acid is one carbon shorter and showed one step less percent mass gain than pentanoic acid in the phase I weight gain study, while acetic acid showed the lowest percent mass gain per concentration in phase 1 of the acid weight gain study, with no significant deviation from water at the lowest concentrations. If butyric is not resolved then it is unlikely that propionic can be, and if acetic is resolved, then it is probable that propionic will be also. The low concentrations were used in the organic acid ageing study, and so accurate and precise weight gain characterization at the low acid concentrations would directly integrate with the results of the organic acid ageing study.

The three PA-11 weight gain experimental approaches were described in Chapter 3. Figures 4.8, 4.9, 4.10, 4.11, 4.12, 4.13, 4.14, 4.15, 4.16, 4.17 and 4.18 show the results for Phase I of the weight gain study (WGS I). Figures 4.19 and 4.20 display the results for Phase II (WGS II). Figure 4.21 displays the results for Phase III (WGS III).

4.2.1 Phase I

Figure 4.8 shows the final volatile content plotted against the number of carbons in the acid side chain per environment. This figure shows that there is a general trend of increased volatile content at varying concentrations with the increasing number of carbon atoms present in the linear acid side chain. The results are exaggerated for higher concentrations of 50% and 75% by volume and imperceptible at the lowest concentrations.

Figure 4.9 shows the percent mass change of grouped PA-11 beads [9] during ageing in acetic acid concentrations plotted against the time aged. This figure shows that there is a relative steady state mass change that is attained within the first ten days of ageing, that higher concentrations of acetic acid result in higher mass changes overall and that at the lowest concentrations there is no perceptible difference from the mass change of 100% water.

Figure 4.10 shows the volatile content change of a PA-11 bead [9] during ageing in acetic acid concentrations plotted against the time aged. The data shown in Figure 4.10 mirrors the data in figure 4.9 and is taken as evidence that the percent volatile content change within the PA-11 matrix directly correlated to the percent mass changes observed.

Figure 4.11 shows the percent mass change of grouped PA-11 beads [9] during ageing in 50% by volume acid concentrations plotted against the time aged. This figure shows both that a steady state is reached in a relatively short period of time, and that the percent mass change is different for the different acids aged at the same concentration.

Figure 4.12 shows the volatile content change of a PA-11 bead [9] during ageing in 50% by volume acid concentration plotted against the time aged. The data shown and observations taken from this figure mirrors that of Figure 4.11.

Figure 4.13 shows the final percent mass change of grouped PA-11 beads [9] during

ageing in 50% by volume acid concentration plotted against the number of carbons in the acid side chain per environment. Isolated to a single concentration, this figure clearly shows that there is a significant trend for increased percent mass gain as the number of carbons in the linear side chain of the acid is increased.

Figure 4.14 shows the final volatile content change of a PA-11 bead [9] during ageing at a 50% by volume acid concentration plotted against the number of carbons in the acid side chain per environment. The data shown and observations taken from this figure mirrors that of Figure 4.13, with the added data points of the propionic acid environment.

Figure 4.15 shows the percent mass change of grouped PA-11 beads [9] during ageing in 75% by volume acid concentration plotted against the time aged. This figure shows greater differences between the different acids than was seen at the 50% by volume acid concentration. The order, increasing with the number of carbons present in the acid side chain, is maintained. However it is of academic curiosity that cyclopropionic acid caused a higher mass gain percentage than pentanoic acid, this was not seen at the 50% concentration. Again, an equilibrium percent mass gain was reached within 10 days and was maintained for each environment.

Figure 4.16 shows the volatile content change of a PA-11 bead [9] during ageing in 75% by volume acid concentration the time aged. This figure mirrors Figure 4.15 in the order of highest relative volatile gained per acid, and an equilibrium percent volatile gain is reached within 10 days for the linear side chain acid environments. However, the data for cyclopropionic acid curiously does not reach an equilibrium, it shows an exaggerated increase in volatile content as the ageing time increases.

Figure 4.17 shows the percent mass change of grouped PA-11 beads [9] during ageing in low acid concentrations plotted against time aged. The data in this figure shows that for the lowest concentrations of 0.06% and 0.36% by volume acetic acid

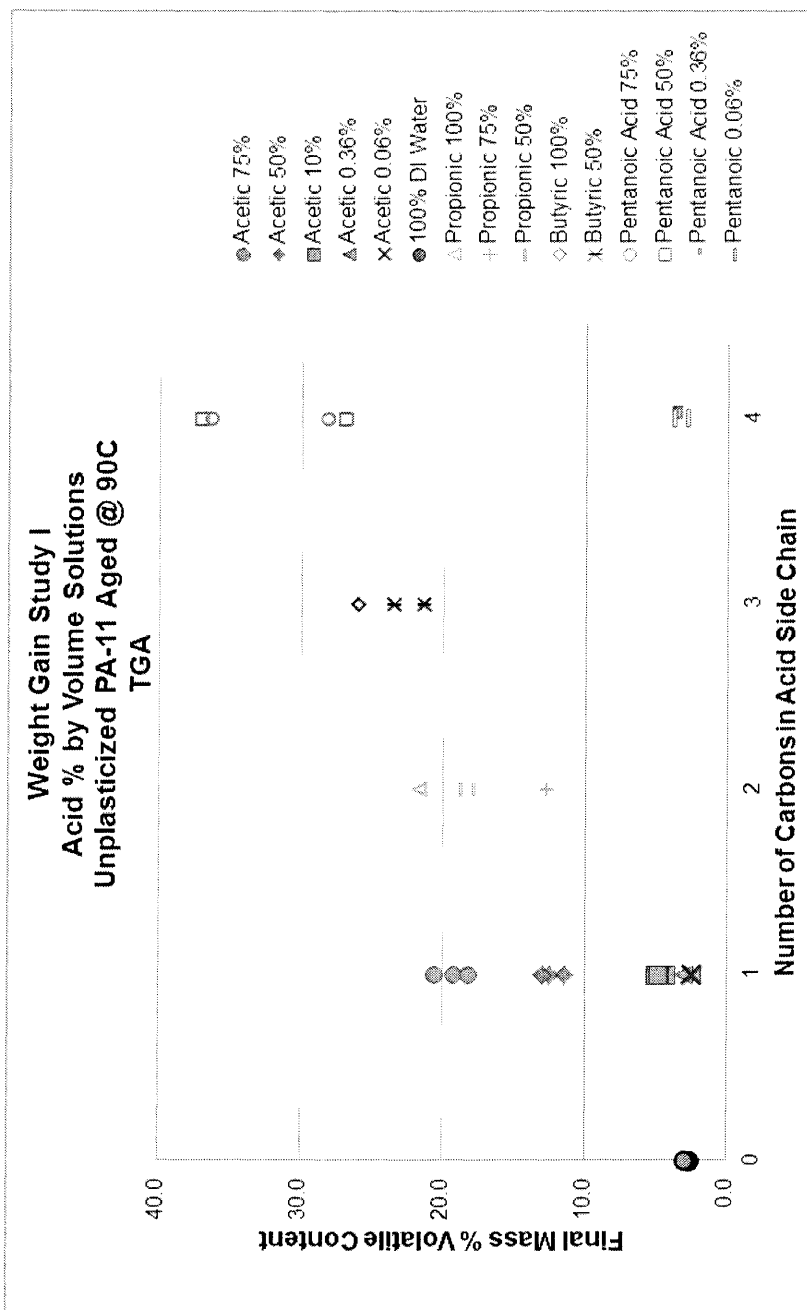
solutions, there is no significant deviation from pure water in the percentage of mass gained by the grouped PA-11 beads. Conversely, there is a significant deviation from water for the grouped PA-11 beads aged at 0.06% and 0.36% by volume pentanoic acid. This supports the findings that longer linear acid side chains in the ageing environment result in higher concentration relative percent mass changes, and also eludes to higher precision measurements needed to examine changes in the PA-11 bead mass when aged at the lowest concentrations of acetic acid.

Figure 4.18 shows the volatile content change of a PA-11 bead [9] during ageing in the low acid concentrations of phase I weight gain study, plotted against time aged. The data shown and observations drawn from this figure mirrors that of Figure 4.17. The resulting desire for higher precision lead to the development of phases II and III of the weight gain study.

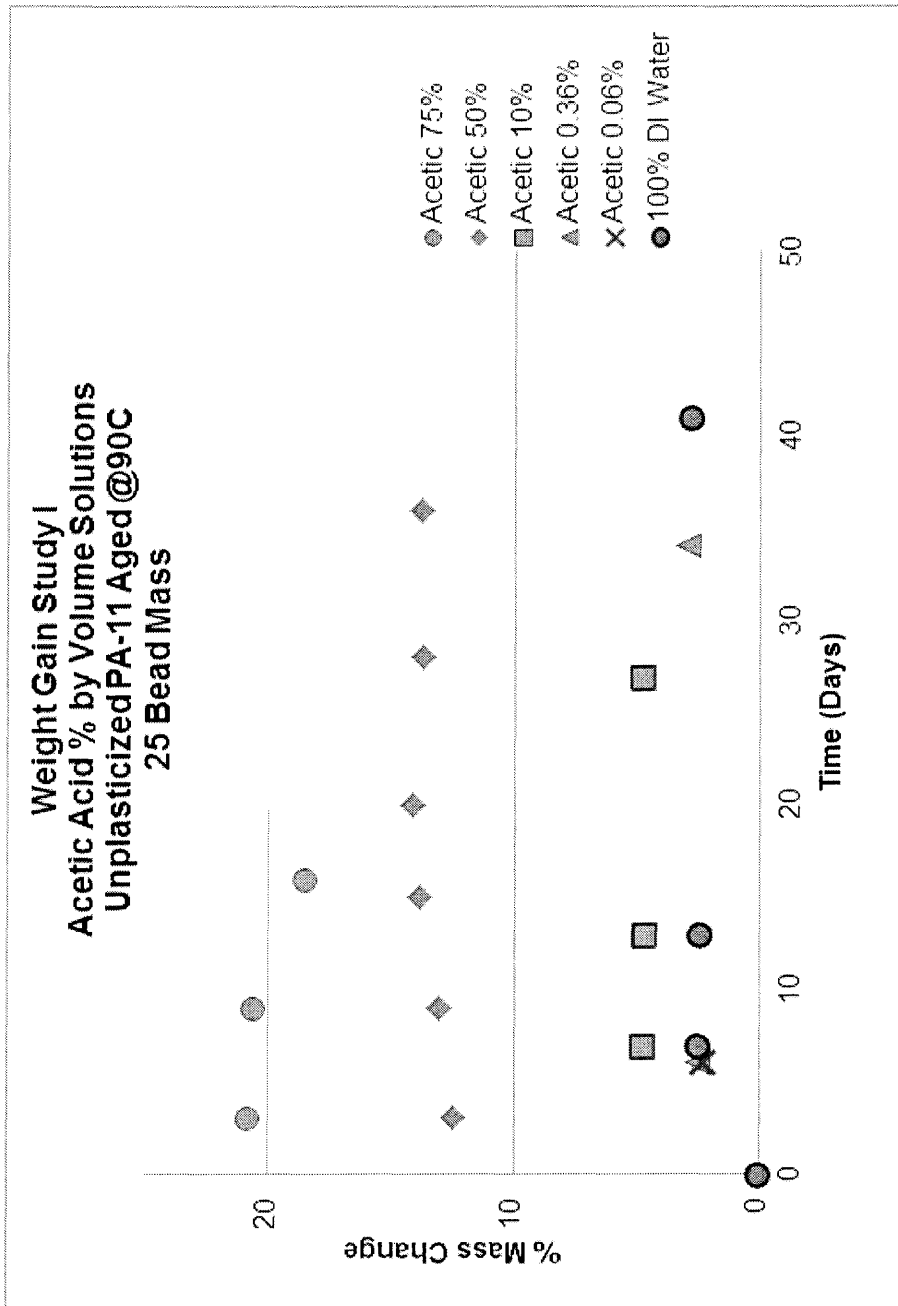
4.2.2 Phase II

Figure 4.19 shows the percent mass change of a single PA-11 bead [9] while aged in low acetic acid by volume concentrations plotted against the elapsed time. The data in this figure shows that there is no significant mass gain deviation for PA-11 aged in acetic acid at low concentrations and pure water.

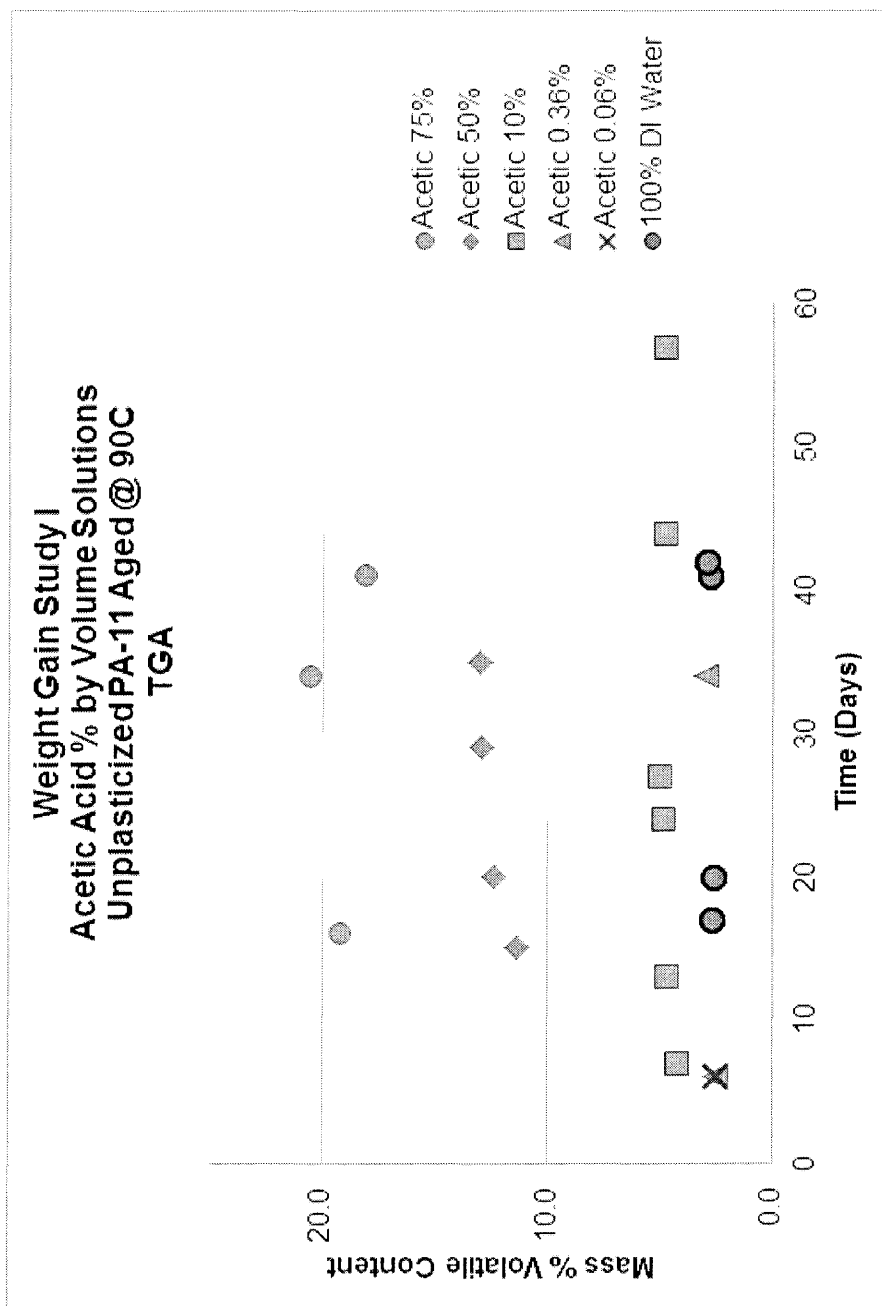
Figure 4.20 shows the percent mass change of a single PA-11 bead [9] while aged in low butyric acid by volume concentrations plotted against the elapsed time. The data in this figure shows that there is no significant mass gain deviation from pure water at the lowest concentration butyric acid solutions. At 10% by volume there is a significant percent mass gain that is in support of higher concentrations producing higher mass gains per carboxylic acid.



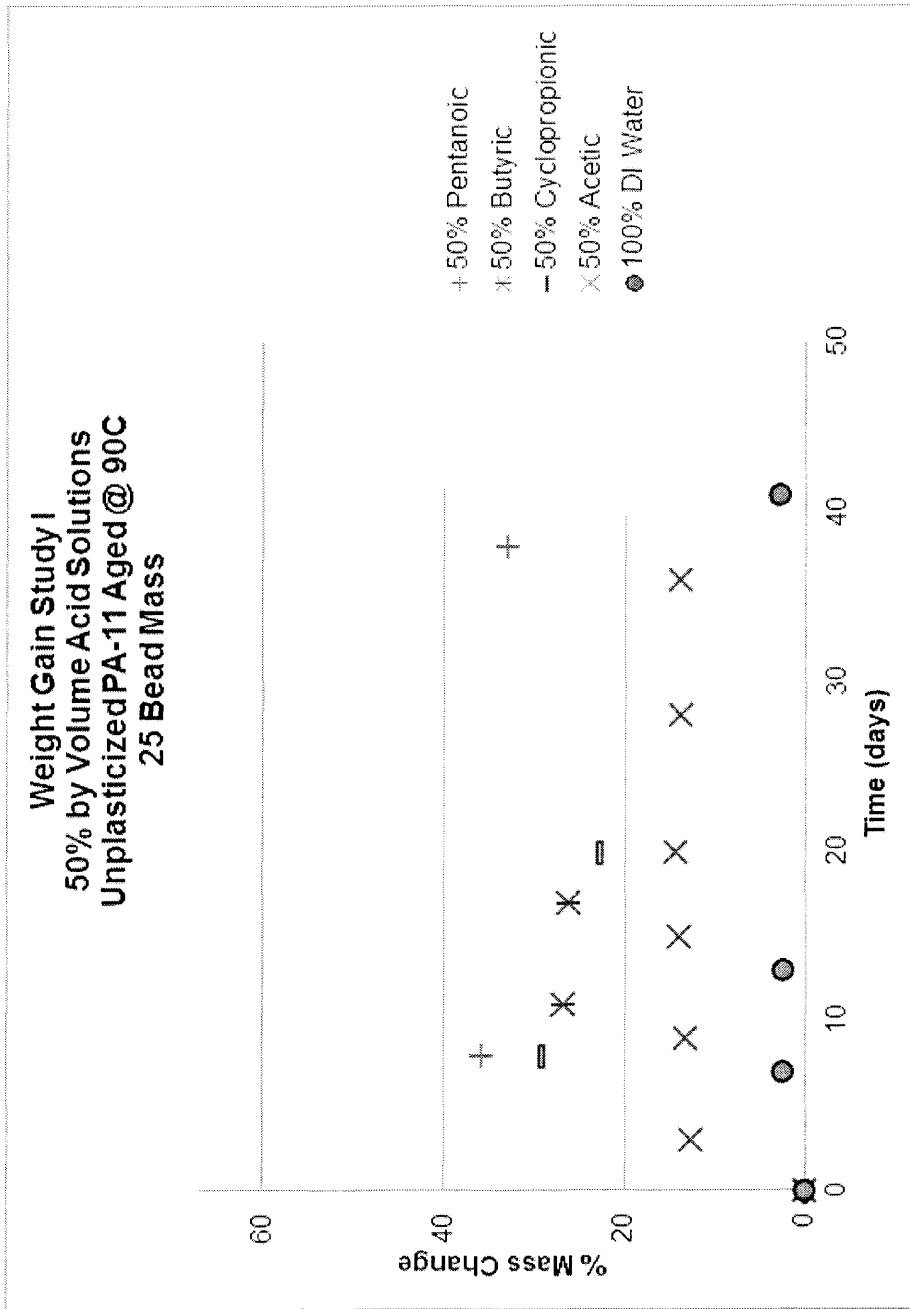
Figures 4.8: WGS I: Final volatile content plotted against the number of carbons in the acid side chain per environment. This study was carried out by ageing unplasticized PA-11 beads [9] in solution at 90°C, and by using the TGA procedure displayed in Table 3.4 monitored the change in volatile content.



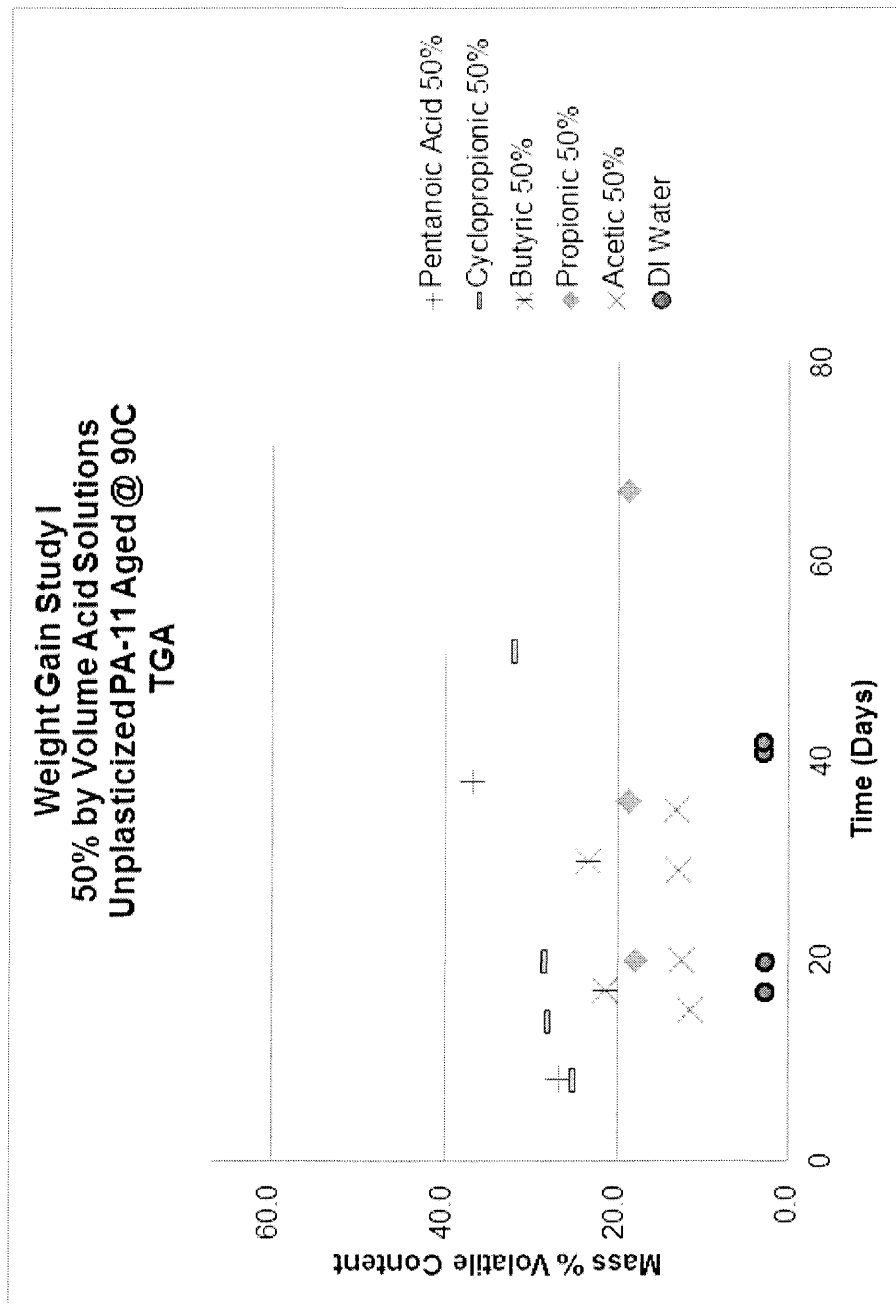
Figures 4.9: WGS I: Percent mass change of PA-11 beads [9] during ageing in acetic acid concentrations plotted against time aged. This study was carried out by ageing unplasticized PA-11 beads [9] in groups of 25 at 90°C, monitoring the change in mass using a balance.



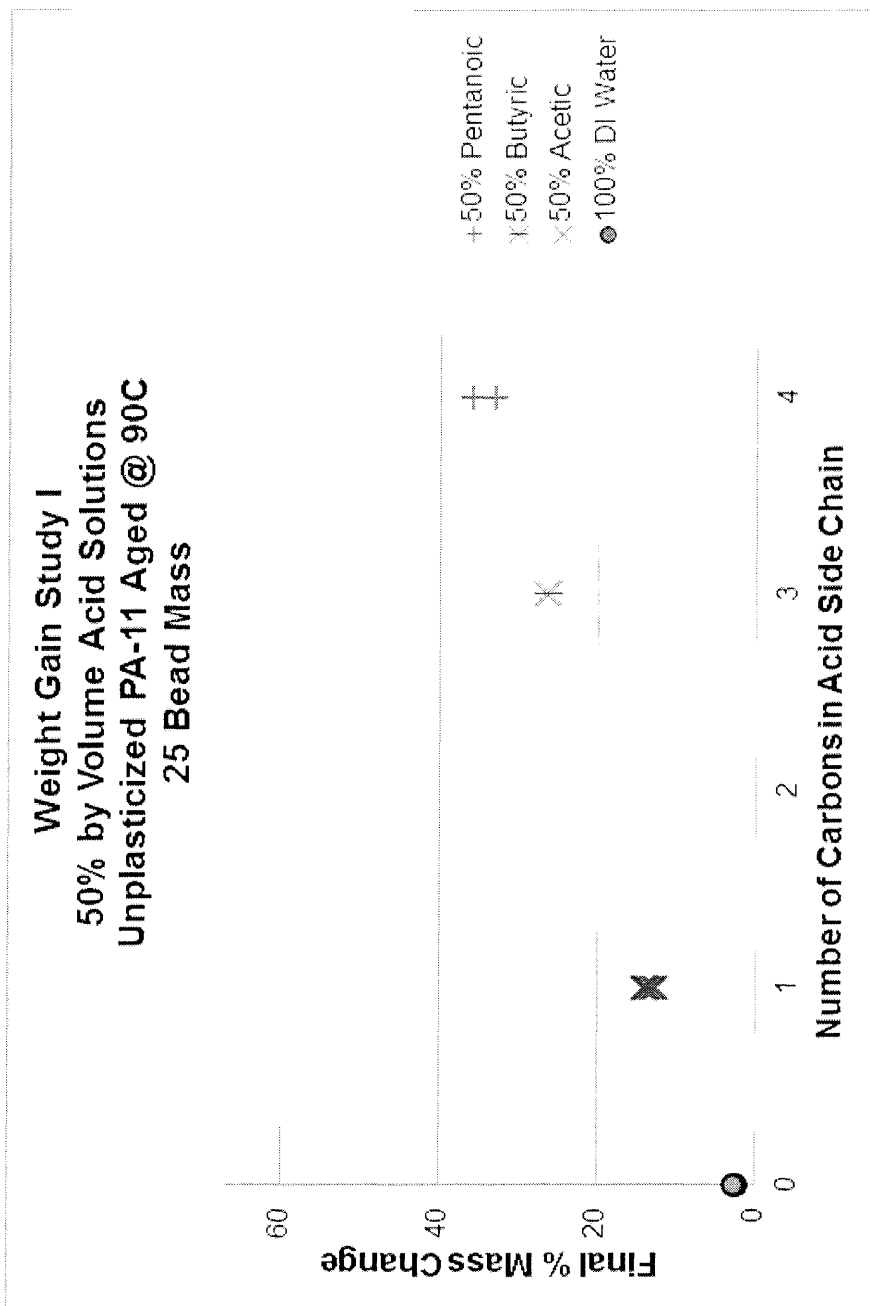
Figures 4.10: WGS I: Volatile content change of a PA-11 bead [9] during ageing in acetic acid concentrations plotted against time aged. This study was carried out by ageing unplasticized PA-11 beads [9] at 90°C, and using the TGA procedure displayed in Table 3.4 monitored the change in volatile content.



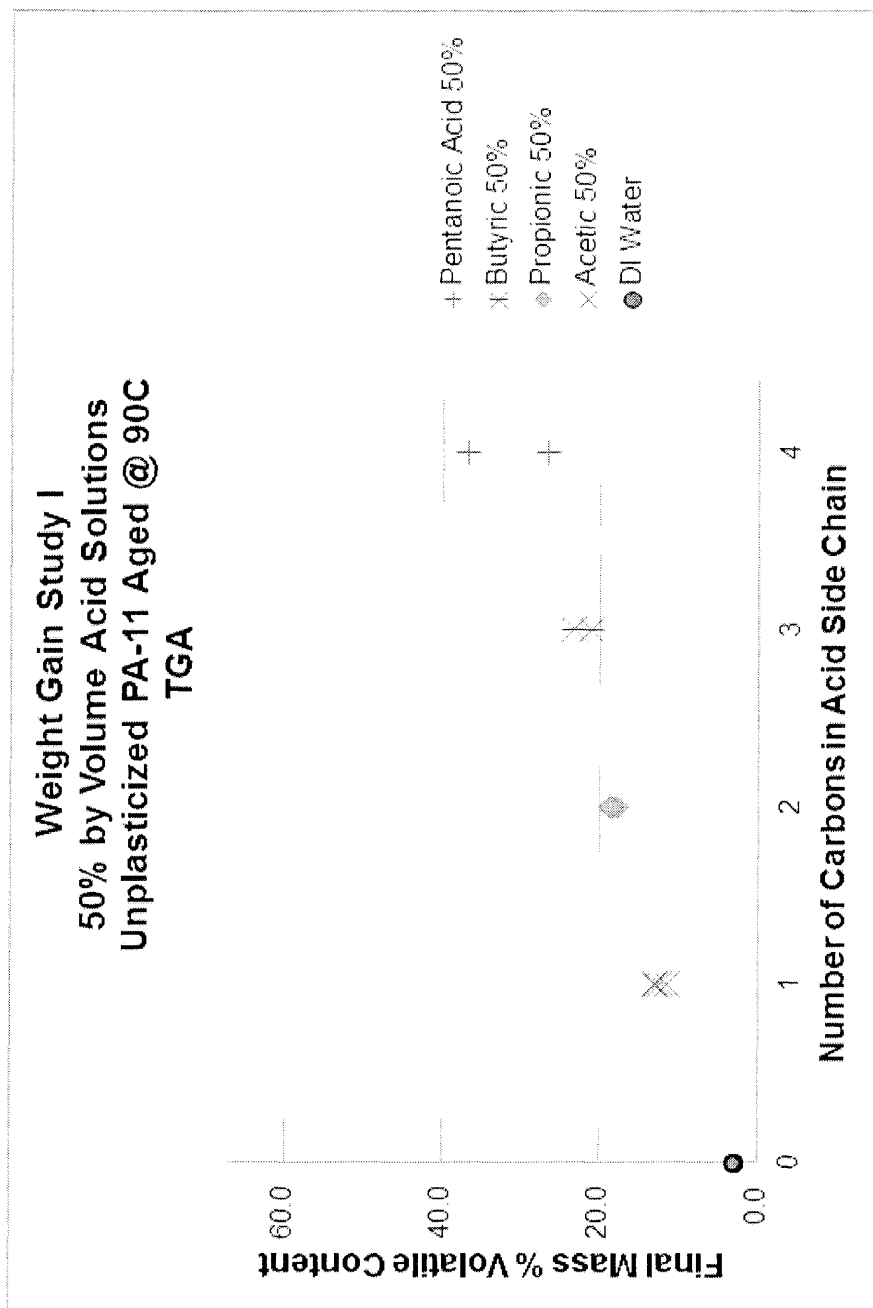
Figures 4.11: WGS I: Percent mass change of PA-11 beads [9] during ageing in 50% by volume acid concentrations plotted against time aged. This study was carried out by ageing unplasticized PA-11 beads [9] in groups of 25 at 90°C, monitoring the change in mass using a balance.



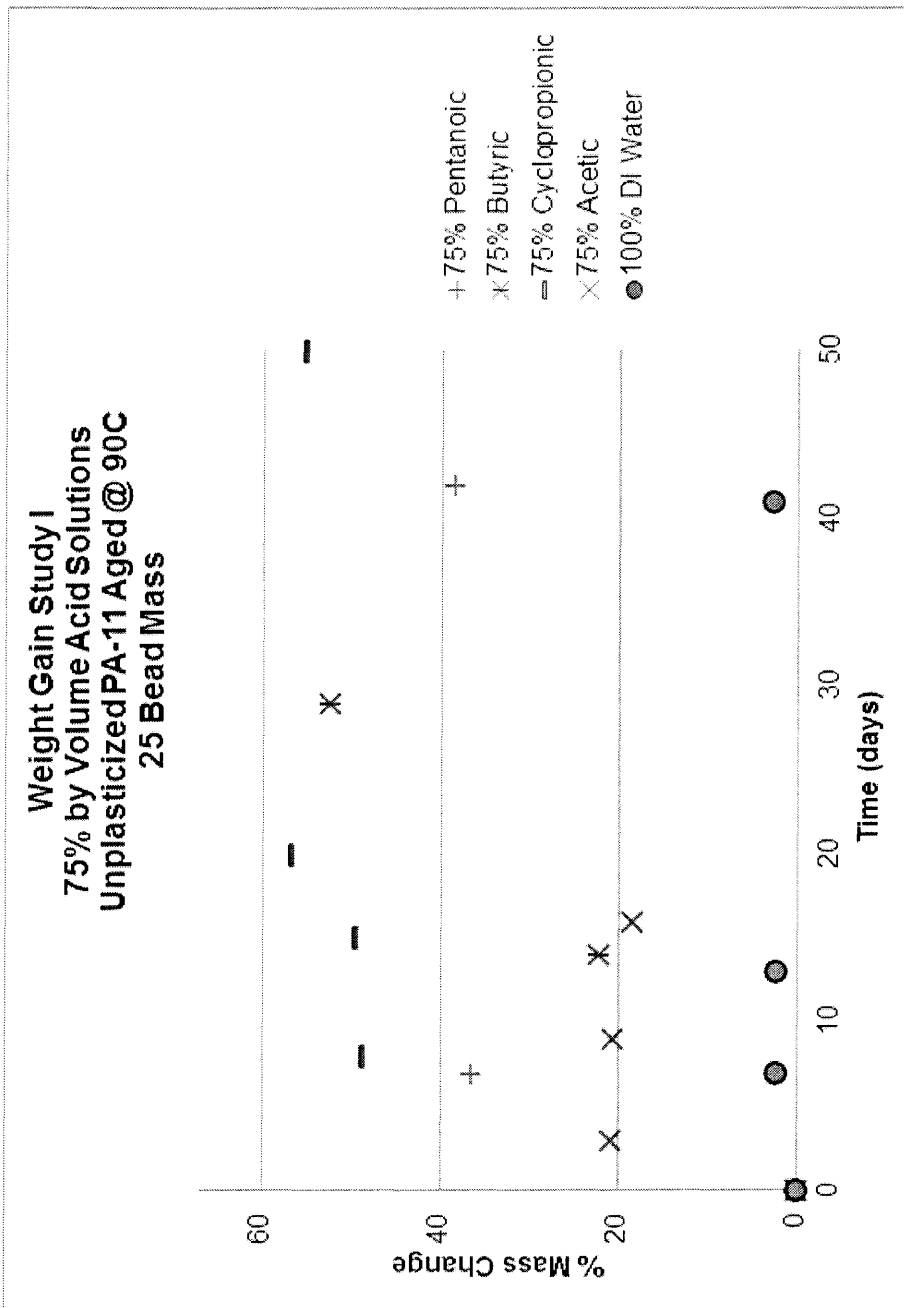
Figures 4.12: WGS I: Volatile content change of a PA-11 bead [9] during ageing in 50% by volume acid concentration plotted against time aged. This study was carried out by ageing unplasticized PA-11 beads [9] at 90°C, and using the TGA procedure displayed in Table 3.4 monitored the change in volatile content.



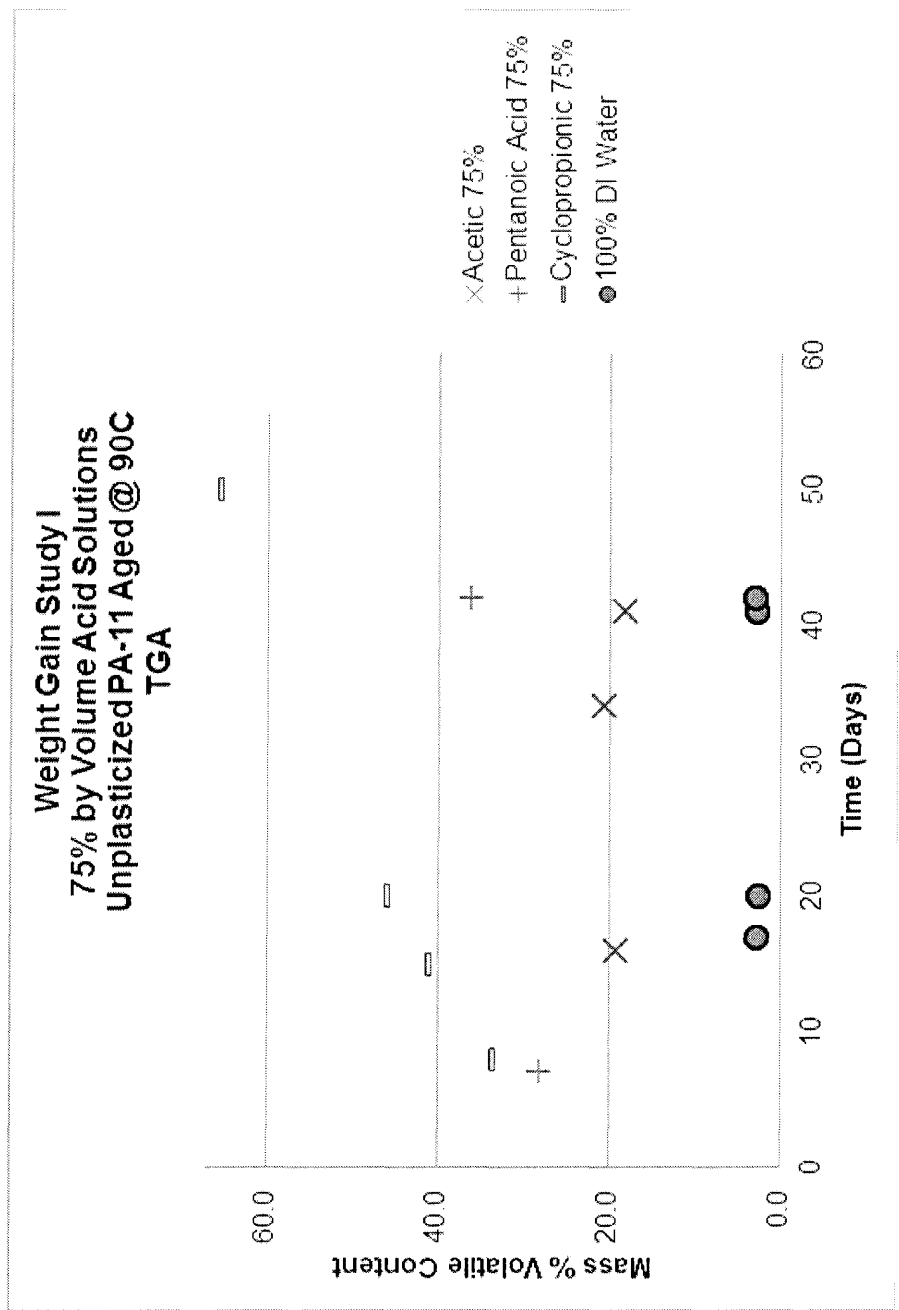
Figures 4.13: WGS I: Final percent mass change of PA-11 beads [9] during ageing in 50% by volume acid concentration plotted against the number of carbons in the acid side chain per environment. This study was carried out by ageing unplasticized PA-11 beads [9] in groups of 25 at 90°C, monitoring the change in mass using a balance.



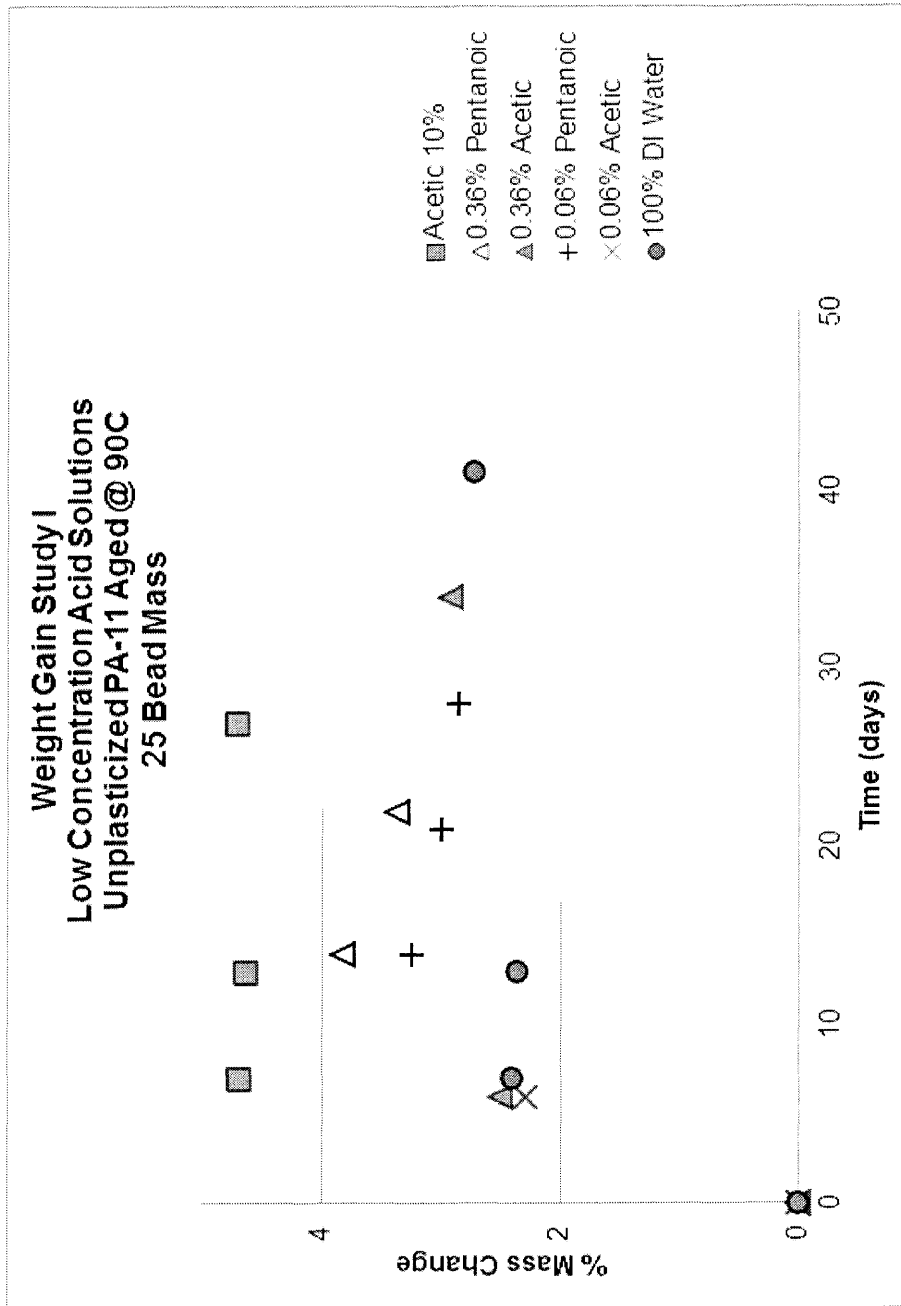
Figures 4.14: WGS I: Volatile content change of a PA-11 bead [9] during ageing in 50% by volume acid concentration plotted against the number of carbons in the acid side chain per environment. This study was carried out by ageing unplasticized PA-11 beads [9] in solution at 90°C, and by using the TGA procedure displayed in Table 3.4 monitored the change in volatile content.



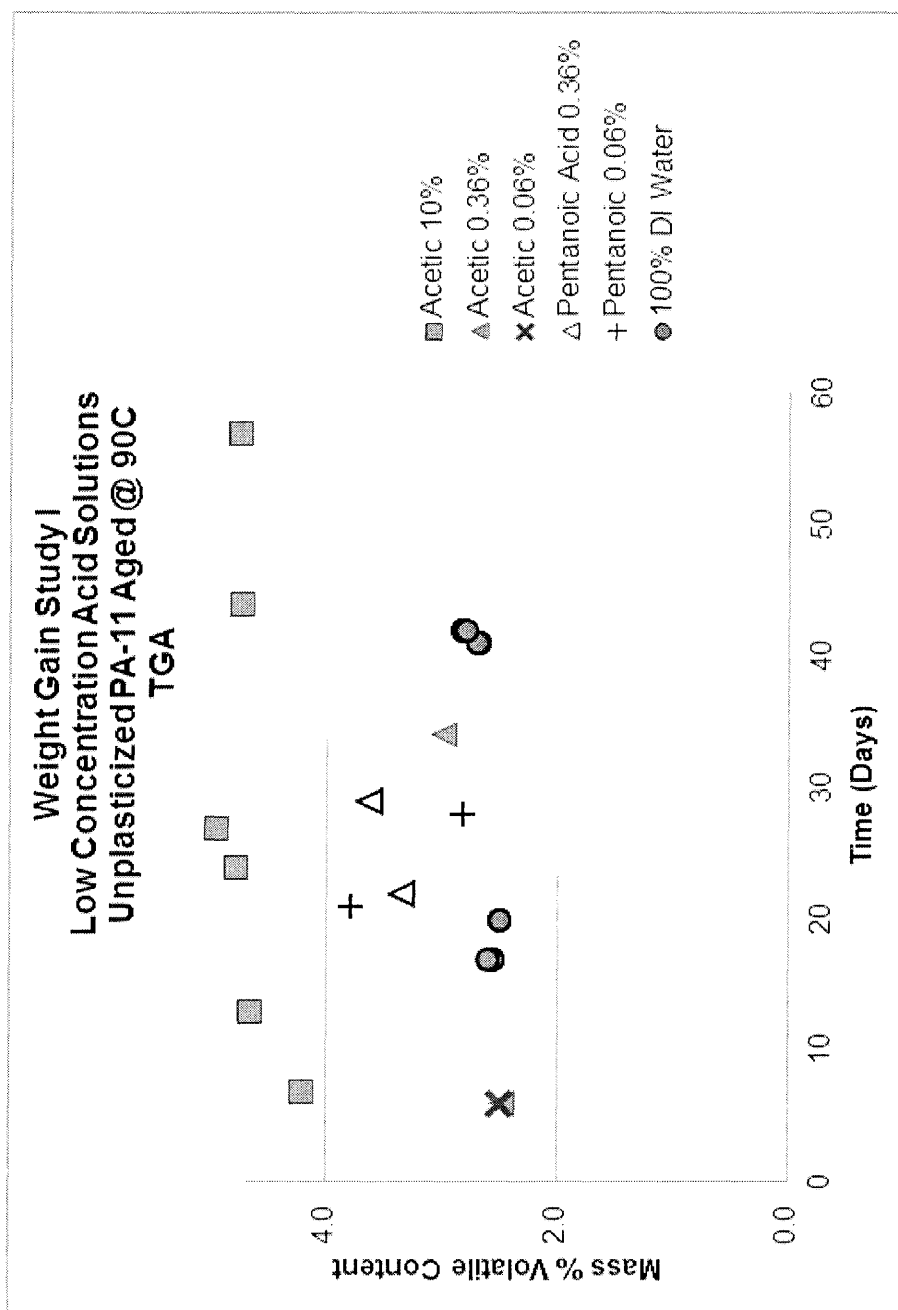
Figures 4.15: WGS I: Percent mass change of PA-11 beads [9] during ageing in 75% by volume acid concentration plotted against time aged. This study was carried out by ageing unplasticized PA-11 beads [9] in groups of 25 at 90°C, monitoring the change in mass using a balance.



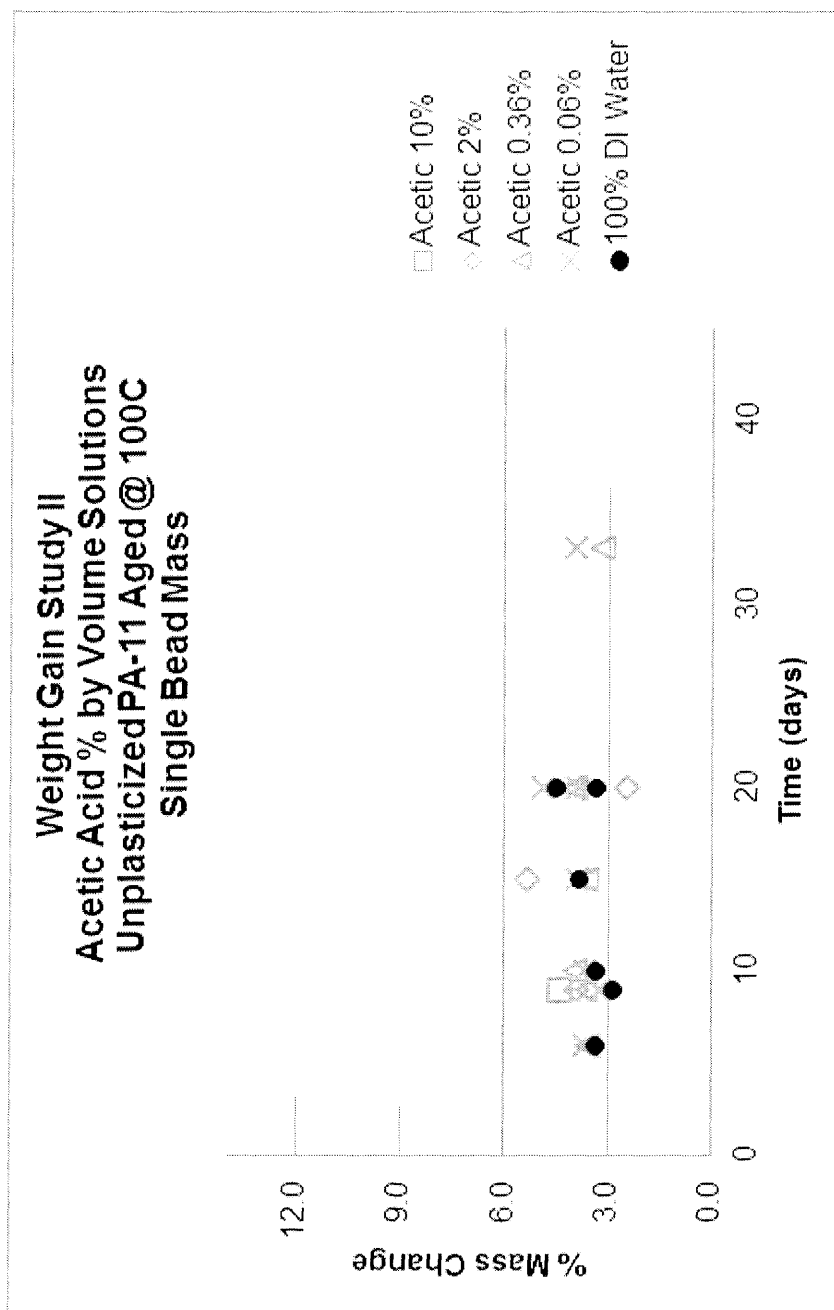
Figures 4.16: WGS I: Volatile content change of a PA-11 bead [9] during ageing in 75% by volume acid concentration plotted against time aged. This study was carried out by ageing unplasticized PA-11 beads [9] at 90°C, and using the TGA procedure displayed in Table 3.4 monitored the change in volatile content.



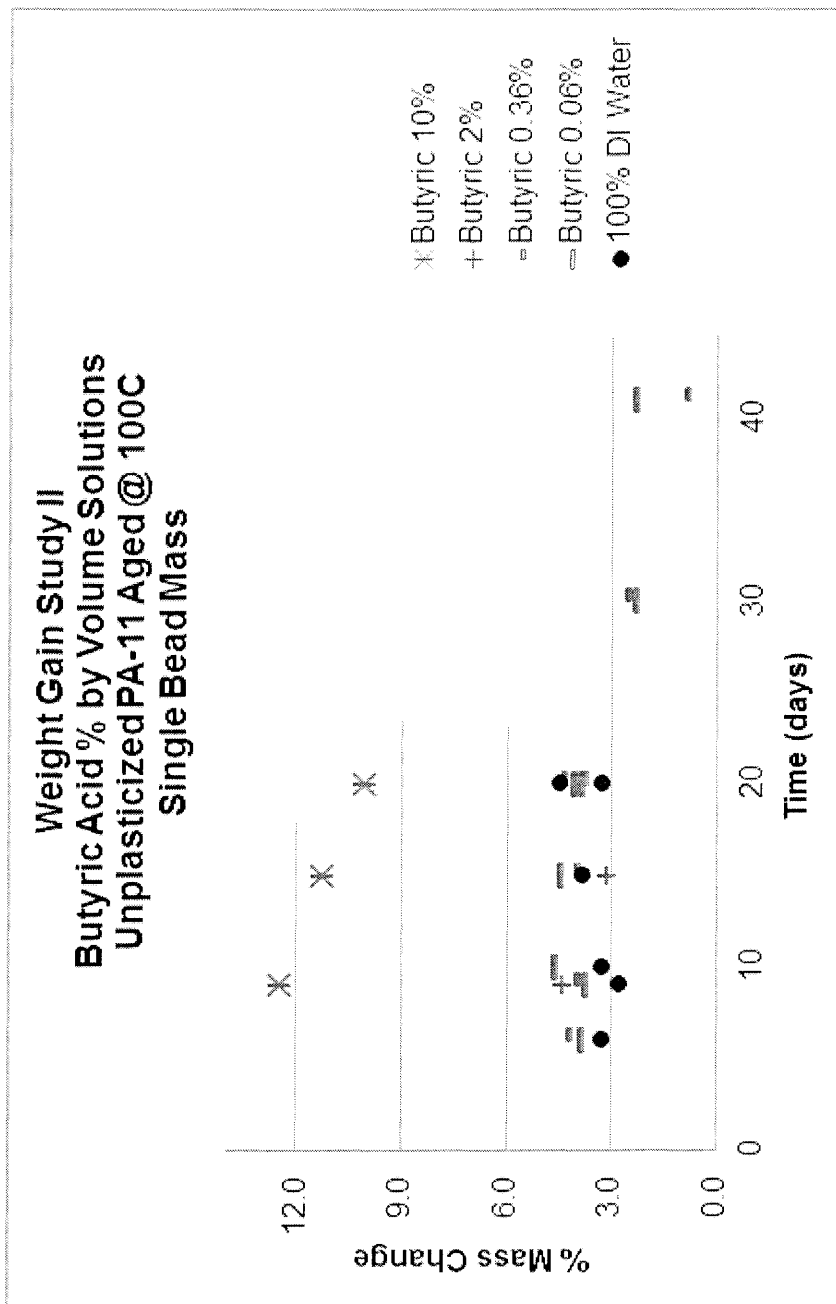
Figures 4.17: WGS I: Percent mass change of PA-11 beads [9] during ageing at low acid concentrations plotted against time aged. This study was carried out by ageing unplasticized PA-11 beads [9] in groups of 25 at 90°C, monitoring the change in mass using a balance.



Figures 4.18: WGS I: Volatile content change of a PA-11 bead [9] during ageing at low acid concentrations plotted against time aged. This study was carried out by ageing unplasticized PA-11 beads [9] at 90°C, and using the thermogravimetric analysis procedure displayed in Table 3.4 monitoring the change in volatile content.



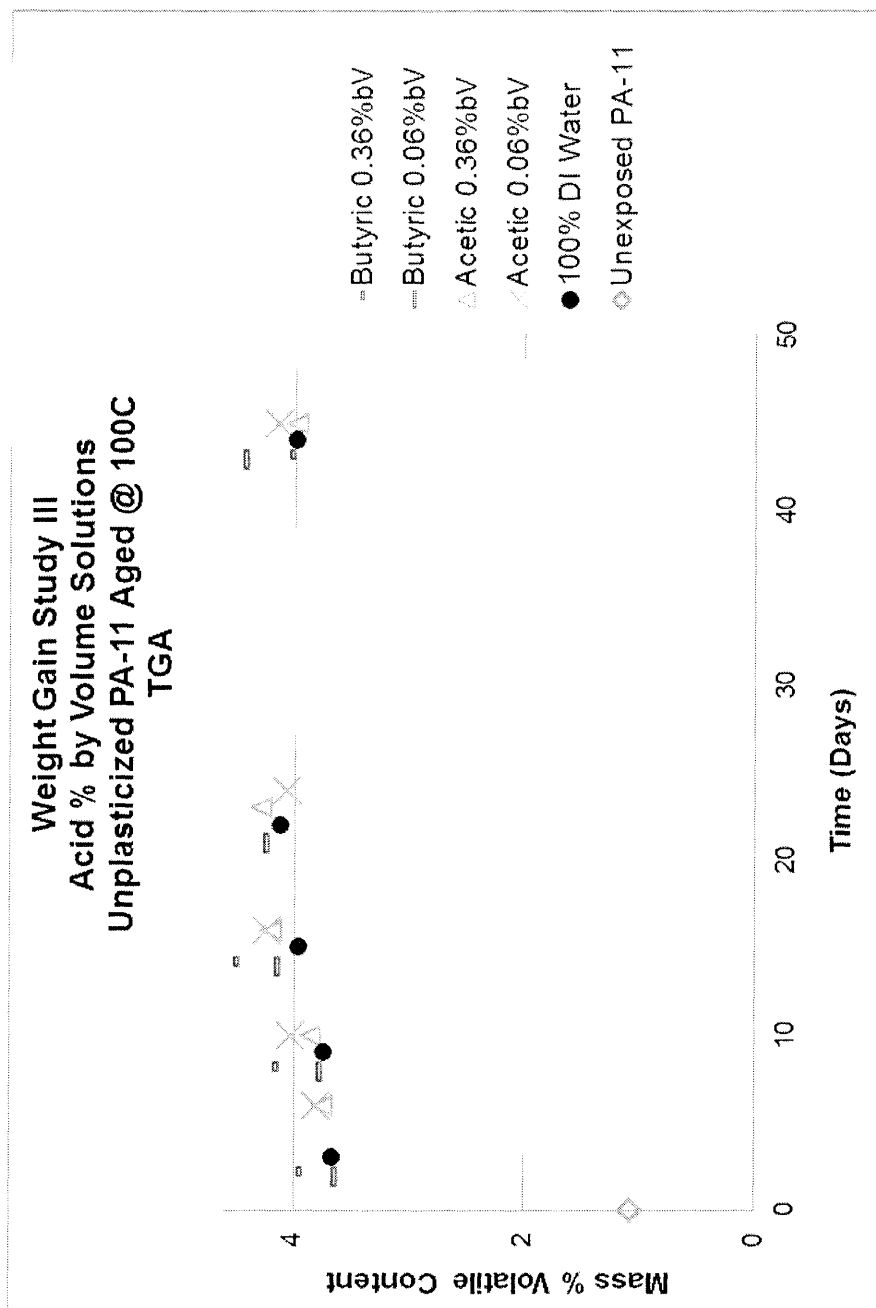
Figures 4.19: WGS II: Percent mass change of a PA-11 bead [9], during ageing in low acetic acid by volume concentrations, plotted against time aged. This study was carried out by ageing a single unplasticized PA-11 bead [9] immersed in 2mL of stock solution at 100°C, monitoring the change in mass using a balance.



Figures 4.20: WGS II: Percent mass change of a PA-11 bead [9], during ageing in low butyric acid by volume concentrations, plotted against time aged. This study was carried out by ageing a single unplasticized PA-11 bead in 2mL of stock solution at 100°C, monitoring the change in mass using a balance.

4.2.3 Phase III

Figure 4.21 shows the volatile content change in PA-11 beads [9] during ageing in acetic and butyric acid at the lowest concentrations plotted against time aged. The data in this figure shows that for PA-11 aged in butyric acid at 0.36% by volume concentration there is a significant deviation from the volatile content change of PA-11 aged in pure water. No significant deviation from the volatile content change of PA-11 when aged in pure water is seen for butyric acid at 0.06%, acetic acid at 0.36% or acetic acid at 0.06%. This result supports the observation that longer linear acid side chains at higher concentrations cause a higher volatile content gain in the PA-11 matrix when aged at elevated temperatures. The inability to observe a gain difference from water at the two lowest concentrations of acetic acid suggests that a more precise method for the measure of absorption into PA-11 is necessary.



Figures 4.21: WGS III: Volatile content change in PA-11 beads [9] during ageing in acetic and butyric acid at low concentrations plotted against time aged. This study was carried out by ageing 3 grams of unplasticized PA-11 beads [9] in 10mL of stock solution at 100°C, and using the Thermogravimetric analysis procedure outlined in Table 2.3 monitored the change in volatile content.

Chapter 5

Discussion

The average molecular weight sample data of the organic acid ageing study were fit using the hydrolysis mathematical model presented in equations 4.2 through 4.12. The hydrolysis kinetic fitting parameters are shown in Table 4.1. The associated hydrolysis prediction lines are plotted through the data in Figures 4.6, 4.4, 4.7 and 4.5.

The number of carbons attached to the carboxyl group is a fundamental difference between the acetic, propionic, butyric and pentanoic acids. In Figure 4.1 the hydrolysis rate constant (k'_H) is shown to increase with the number of carbons in the acid side chain. In Figure 4.3 the M_{We} is shown to be lower for the higher counts of carbons in the acid side chain. The trend for the recombination rate constant (k_R) as plotted in Figure 4.2 is not monotonic with respect to the hydrolysis rate constant or the equilibrium molecular weight. The initial assumption is that these kinetic parameters are a result of the pH of the solution in which the sample was aged. It is shown that there is no correlation between the initial assumption and the experimentally determined hydrolysis kinetics of the organic acid ageing study.

Figure 5.1 provides a qualitative comparison of the calculated environmental pH relative to the acid chain length. Note that pentanoic acid only has modest solubility in water at room temperature. However, in a previous organic acid ageing study, no difference in the hydrolysis kinetics of PA-11 aged in the water or mineral oil layer was

found for all acid environments examined, including pentanoic 0.06% and 0.36% [4]. Consistent with efficient phase transfer catalysis under the experimental conditions, for this qualitative comparison it was assumed that all the acids were equally distributed between the organic and aqueous phases at 100 °. The established mechanism for acid catalyzed hydrolysis, Figure 5.2, requires the presence of a disassociated hydrogen to proceed [10]. Acid dissociation in mineral oil is negligible. To compare the relative pH per ageing environment the pH of the aqueous solutions was calculated assuming dissociation based on each acid's pKa (Table 3.1). The concentration of acid in the aqueous phase was estimated to be half the total concentration, Appendix A.

To address the initial assumption that the equilibrium hydrolysis parameters would be a result of the solution pH, Figure 5.1 is presented. For each environment of the organic acid ageing study, the true internal pH is taken to be proportional to the calculated pH of the initial acid solution. The resulting comparison (Figure 5.1) includes the calculated pH of the eight acid solutions: acetic, propionic, butyric and pentanoic at 0.06% and 0.36% by volume for a qualitative comparison of expected versus experimental results.

We hypothesized the kinetics of PA-11 hydrolysis per acid molecule concentration will vary according to the acid side chain structure. To clarify the basis for a structural role of the organic acid during hydrolytic ageing of PA-11, the pH for each acid solution is plotted against the number of carbons in the varying acid side chains (Figure 5.1). The relationship between the experimental hydrolysis kinetics and the calculated pH per solution is unanticipated for the individual acids under the initial assumption. Acid catalyzed hydrolysis relates a higher pH to a lower hydrolysis rate constant (k'_H) and higher equilibrium molecular weight (M_{We}). At a given concentration the calculated solution pH is shown to increase with the increasing number of carbons; but the corresponding k'_H is shown to be higher with the M_{We} being lower. The results of

the organic acid ageing study are not correlated to the expected outcome of the initial assumption. Therefore, it is deduced that the pH of the carboxylic acid solution has a negligible effect during the hydrolysis reaction, and that the equilibrium hydrolysis kinetics are determined by the acid side chain structure. Our hypothesis was supported by the experimental results.

Given the results of the organic acid ageing study, the mechanistic action governing the differences in hydrolysis kinetics per acid side chain structure remains undeveloped. Two potential explanations are offered to address this phenomenon:

- 1) The relative solubility between the different acids and the PA-11 matrix affects their presence inside the polymer and thus the likely-hood that they can promote acid catalyzed hydrolysis from within the polymer matrix.

- 2) The entropy of the system paired with the excluded volume differences associated with each acid, such that once the molecule is incorporated into the PA-11 matrix it leads to energetically favourable orientations of the carboxylic acid end group with amide bonds within the PA-11 matrix.

Three phases of a weight gain study were implemented to address solubility of the varying acids into the PA-11 matrix as a plausible explanation for the mechanistic action governing the hydrolysis rate results found in the organic acid ageing study.

In the weight gain study, it was hypothesized that higher concentrations and longer linear side chain acids will show preferential mass gain or volatile content gain in the PA-11 matrix. The weight gain study results show a trend of higher mass and higher volatile content correlated to higher concentrations and the higher number of carbons in the carboxylic acid linear side chain. The weight gain study examined how unplasticized PA-11 [9] aged in varying small carboxylic acid containing environments. This trend persists for all acids studied in WGS I and butyric acid in WGS II. The results of WGS II did not show significant differences between the 0.36% and 0.06%

concentrations, nor side chain structure. The results of WGS III showed significantly higher volatile content for the 0.36% over the 0.06% concentration of butyric acid. There was no difference between acetic acid and deionized water at the concentrations of 0.36% and 0.06% for WGS I, WGS II or WGS III. Our hypothesis was supported by the experimental results.

As a partial explanation of the organic acid ageing study and the weight gain study results, the relative cohesion interactions between each of the acids and the PA-11 matrix is examined. The Hildebrand solubility parameter or total cohesion parameter (δ_t , equation 5.1) is an approach to qualitatively estimate the favourable mixing of two materials at a given temperature. The fundamental theory of δ_t is founded on the relationship between the internal energy (U) and the molar volume (V) of each molecule. This theory has been extended to account for the various other chemical properties a given molecule possesses, such as: Van der Waals interactions, Lewis acid or base, hydrogen bonds, et alii. The cohesion parameter theory is applied such that for a material with a high δ_t value more energy is required to disperse amidst a material having a low δ_t than is gained from the resulting entropy. Conversely, sufficient energy being gained through mutual dispersal of two materials having a similar δ_t harkens the likely miscibility of the two. [7]

$$\delta_t = \left(-\frac{U}{V}\right)^{\frac{1}{2}} = \left[\frac{RT\rho}{M} \left(1 - \frac{pT_C^3}{p_C T^3}\right)^{\frac{1}{2}} \frac{2.303BT^3}{(T + C - 273.16)^2} - 1 \right] \quad (5.1)$$

In equation 5.1: U is the molecular internal energy, V is the molar volume, R is the gas constant ($8.314 \frac{\text{Joules}}{\text{mole} \times \text{Kelvin}}$), T is the temperature (kelvin), ρ is the molecules' density ($\frac{g}{mL}$), M is the molecular weight ($\frac{g}{mole}$), p is the vapour pressure (MPa), T_C is the critical temperature, p_C is the critical vapour pressure, B and C are constants from the Antoine equation. The Antoine equation was used in conjunction with an empirically derived extrapolation of the vaporization enthalpy at 25 °C to define the

vapour pressure for a given system [7]. The δ_t 's for acetic, propionic, butyric and pentanoic acids, as derived using equation 5.1, are tabulated in Table 5.1.

A polymer's cohesion parameter is empirically derived. An array of good solvents are determined for the given polymer. A good solvent is a solvent in which the polymer chain can expand. In a good solvent, the interactions between the polymer and the solvent are energetically favourable. From the array of good solvents, the best solvent is determined. The best solvent is the one that maintains the highest concentration of polymer chains of a given size at a specific temperature. The δ_t of the best solvent is taken to be the δ_t of the polymer [23]. The total cohesion parameter for PA-11 is listed in Table 5.1.

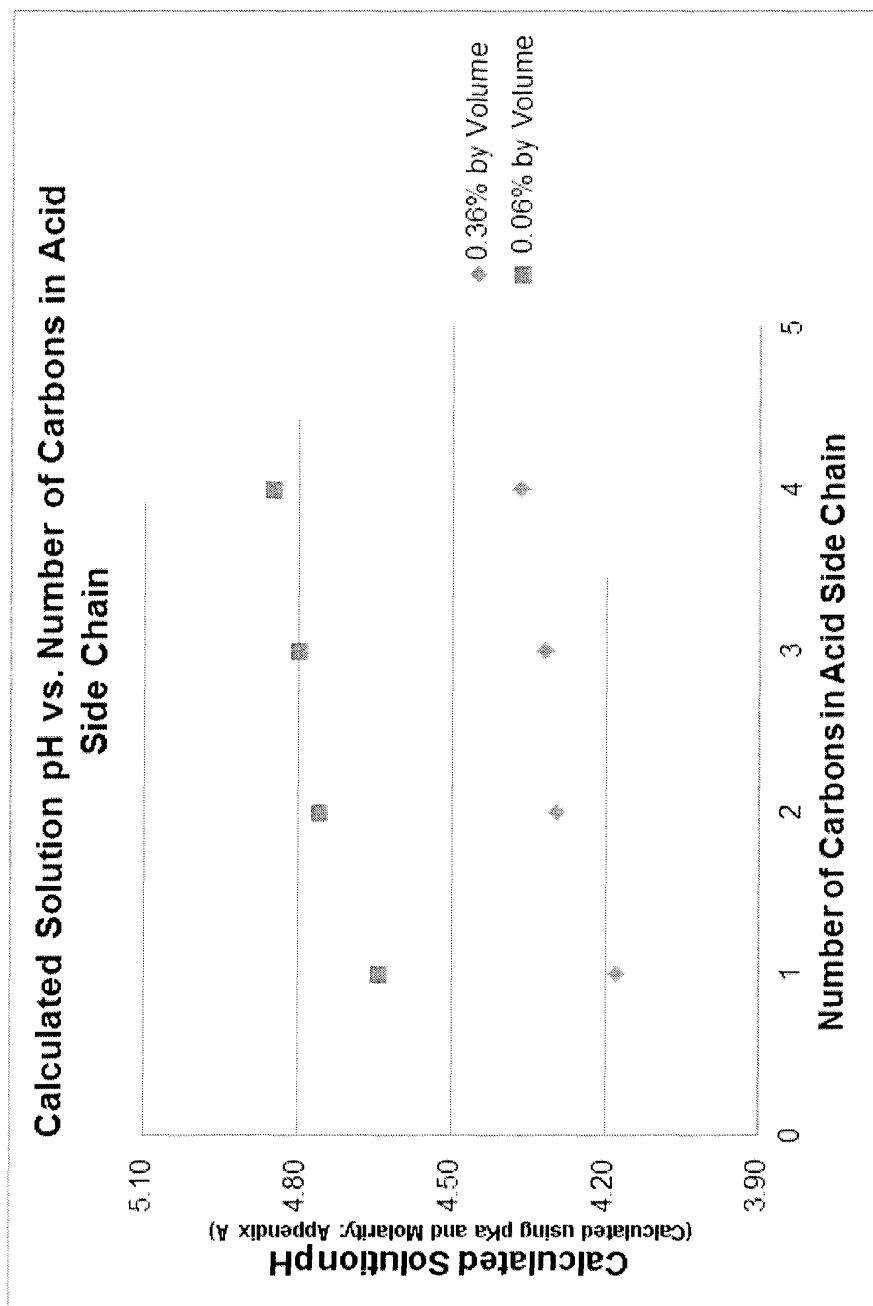
Linear Carbons	Sample Name	Solubility Parameter (δ) MPa ^{1/2}
	Poly(amide) 11	19.2
1	Acetic Acid	26.5
2	Propionic Acid	25.5
3	Butyric Acid	24.5
4	Pentanoic Acid	24.0

Tables 5.1: Solubility parameters δ at standard conditions [6] [7]

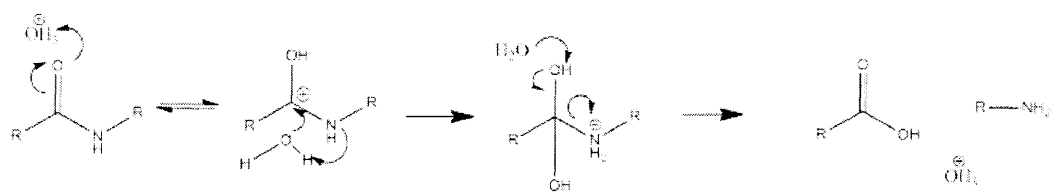
By examining qualitative comparison of the k'_H values (Figure 4.1) and the weight gain results (Figures 4.8, 4.13 et al.) to the differences between the acids solubility parameters and the PA-11 solubility parameter (Figure 5.3) a correlation is seen. As a guideline, when two solubility parameters are more similar, it is more likely they will be miscible with one another. It is shown in Table 5.1 that the solubility parameter of the given acid gets closer to the solubility parameter of PA-11 as the number of carbons in the acid side chain increases. The likelihood for favourable solubility is seen by plotting the reciprocal of the square of the difference between the solubility parameters of PA-11 and the linear side chain acid against the number of carbons in the linear acid side chain

(Figure 5.3). The increasing closeness of the Hildebrand solubility parameters for each of the acids with increasing number of carbons in the side chain of the acid to that of PA-11's Hildebrand solubility parameter agrees with the weight gain study results as well as the hydrolysis kinetics found in the organic acid ageing study. This qualitative correlation suggests that solubility should be accounted for when developing a model for the results of the organic acid ageing study and the weight gain study.

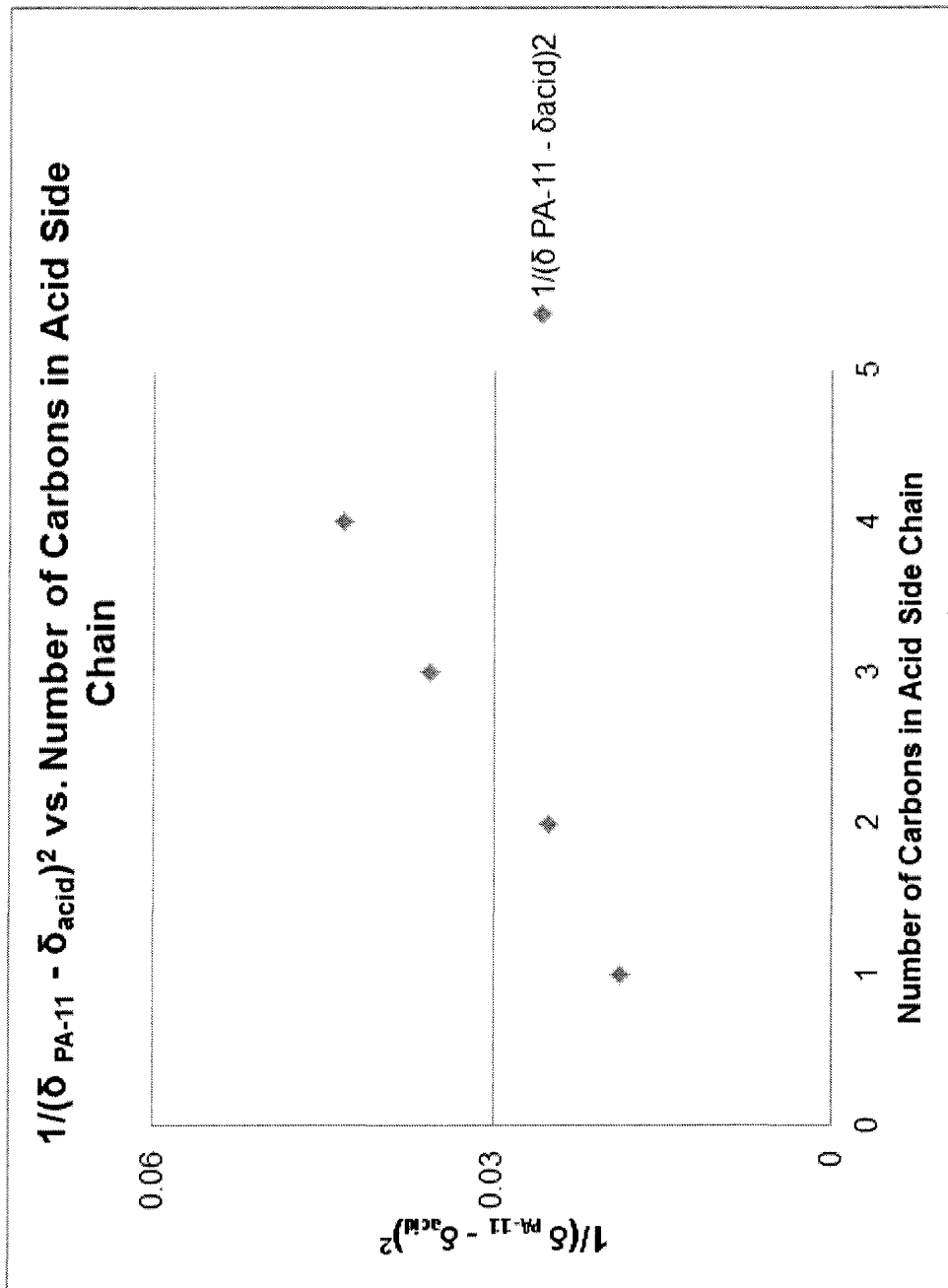
The experimental results of the organic acid ageing study showed that different organic acid structures present in the solutions exhibited different k'_H 's and M_{We} 's that correlated directly to mass and volatile gain of PA-11 when submerged in the solutions. The evidence presented shows that the concentration of the acid within the PA-11 polymer matrix drives a higher k'_H and a lower M_{We} when aged in acid solution.



Figures 5.1: Calculated acid solution pH plotted against the number of carbons in the acid side chain.



Figures 5.2: The mechanism for acid catalyzed hydrolysis of an amide bond. [10]



Figures 5.3: The reciprocal of the square of the difference between the solubility parameters of PA-11 and the linear side chain acids plotted against the number of carbons in the linear acid side chain.

Chapter 6

Conclusion

The work presented in this thesis shows that there exists a strong correlation between the accelerated ageing, the number of carbons in the carboxylic acid side chain, the mass and volatile content change of PA-11 when exposed to various organic acid environments. In the organic acid ageing study it has been shown that the kinetics of PA-11 hydrolysis per acid varied according to the acid hydrocarbon chain structure. The reason for the varying hydrolysis kinetics of PA-11 per acid is the concentration of the acid in the polymer matrix. The pH of the solution has been shown to play no significant role. The weight gain studies have shown that for the higher solution concentrations and longer linear side chain carboxylic acids, there were higher mass and volatile gain in unplasticized PA-11 [9]. The results were correlated to the Hildebrand solubility parameter differences between the acids and PA-11. Further examination of this phenomena would be necessary before a mechanistic model can be presented.

Chapter 7

Future Work

In order to clearly elucidate a working model for the results of the organic acid ageing study and the weight gain study the following proposed work would be essential:

The preferential absorbency of water or acid from solution into the polymer matrix needs to be ascertained. Preferential solubility of acid or water from solution into the PA-11 matrix could be monitored by: placing 3 grams of PA-11 polymer into an acidic solution (sparged of oxygen), and elevating the temperature for a determined time period, extracting a sample and using a TGA to determine changes in the PA-11 volatile content with a simultaneous IR analysis of the volatiles to determine composition. Another option could be to monitor the solution changes via pH titration, gas chromatography (GC) or mass spectrometry (MS).

The diffusion rate of the various carboxylic acids through the PA-11 matrix at varying solution concentrations needs to be determined. This can be done by placing 1 cm³ pieces of PA-11 into pressure tubes with known concentrations of the various acids. Using a method consisting of uniformly shaped samples, pre-determined pulls, single sample per tube, set temperature of 100 °C, pH of solution titrated before ageing and per pull, standard measure and method of slicing each sample, standard placement per slice to measure TGA-IR and SEC-MALLS, argon sparge per tube. Attaching the TGA to the IR may be useful, it is possible that it will show on the IR spectra when

the acid is present per slice of the sample. The SEC-MALLS will measure perceptible changes in the average molecular weight per slice which would indicate hydrolysis rate changes, a qualitative measure of the aqueous diffusion.

Finally, the varying potential for these small organic carboxylic acids to react with the amide group during hydrolysis of the amide bond needs to be explored. When this happens the question arises at the scission point: is there an energetically favoured condensation among the different acids with the hydrolysed amide or is recombination favoured. A dispersion of the monomer in varying acid solutions could be the phase 1 study. Qualitatively: products could be monitored using titration of the solution pH or liquid chromatography. Quantitatively: the products could be monitored via GC and MS. As a phase 2 study, the change in pH of a closed system at elevated temperatures both with the polymer absent and present during the ageing process would be monitored. This could be done using three control tubes: a tube with only water, with water and polymer, with only acid, with polymer and acid. Each tube would be sparged of oxygen using Argon. Once sealed, each tube would be sampled for 5 mL of solution. Using GC/MS and titrating the pH, the deviation from the polymer absent and polymer-water environments would be examined. The SEC-MALLS would be used to examine the differences in the average molecular weight of the polymer for each sampling.

Bibliography

- [1] Andrew Meyer; Nick Jones; Yao Lin; David Kranbuehl. Characterizing and modeling the hydrolysis of polyamide-11 in a pH 7 water environment. Macromolecules, 35(7):2784–2798, 2002.
- [2] N. Chaupart; G. Serpe; J. Verdu. Molecular weight distribution and mass changes during polyamide hydrolysis. Polymer, 39:1375–1380, 1998.
- [3] B. Jaques; M. Werth; I. Merdas; F. Thominet; J. Verdu. Hydrolytic ageing of polyamide 11. 1. hydrolysis kinetics in water. Polymer, 43:6439–6447, 2002.
- [4] Arthur Jaeton Mitman Glover. Characterization of PA-11 Flexible Pipe Liner Aging in the Laboratory and in Field Environments Throughout the World. Phd dissertation, The College of William and Mary, Williamsburg, VA, 2011.
- [5] Robert Weast, editor. Handbook of Chemistry and Physics. The Chemical Rubber Company, Cleveland, OH, 51 edition, 1971.
- [6] J. Brandrup; E. H. Immergut; E. A. Grulke. Polymer Handbook, 4th Edition. John Wiley and Sons, New York, NY, 4 edition, 1999.
- [7] Allan F.M. Barton. Handbook of Solubility Parameters and Other Cohesion Parameters. CRC Press, Inc., Boca Raton, FL, 1983.
- [8] NKT. <http://www.nktflexibles.com/en/products+and+solutions/materials+and+profiles.htm>. Riser design and Product information, January 2012.
- [9] Aldrich. Nylon 11. unplasticized 25035-04-5.
- [10] Dirk Zahn. On the role of water in amide hydrolysis. European Journal of Organic Chemistry, pages 4020–4023, May 2004.
- [11] ExxonMobil. Statement to the National Commission on the BP Deepwater Oil Spill and Offshore Drilling. http://www.exxonmobil.com/Corporate/news_speeches_20101109_rwt.aspx, November 2010.
- [12] NKT. <http://www.nktflexibles.com/en/projects/nkt+project+references.htm>. Project References, January 2012.

- [13] Leslie Howard Sperling. Introduction to Physical Polymer Science. John Wiley and Sons, Hoboken, NJ, 4 edition, 2006.
- [14] I. Merdas; F. ThomINETTE; J. Verdu. Hydrolytic ageing of polyamide 11-effect of carbon dioxide on polyamide 11 hydrolysis. Polymer Degradation and Stability, 79:419–425, 2003.
- [15] Showa Denko K. K. Operation Manual for Shodex PAK GPC HFIP-800 Series. Showdex (Seperation & HPLC) Group, Tokyo, Japan, shodex operation manual no. 840 edition, 2010.
- [16] Zimm. Apparatus and methods for measurement and interpretation of the angular variation of light scattering; preliminary results on polystyrene solutions. Journal of Chemical Physics, 16(12):1099–1116, 1948.
- [17] Wyatt Technologies Corporation, editor. DAWN, miniDAWN and Optilab Applications, MiniDAWN, Santa Barbara, CA, 1999. Light Scattering University.
- [18] Supelco Analytical. Frits, 2um x 1/8" OD. Bellefonte, PA, 2011. Product number: 59129.
- [19] Wyatt Technology Corporation. Manual for miniDAWN Light Scattering Instrument. Wyatt Technologies, Santa Barbara, CA, May 1998.
- [20] American Petroleum Institute. Api technical bulletin tr17rug, 1st edition. Bulletin TR17RUG, API, June 2002.
- [21] Eutech Instruments. Oakton Portable DO Meter. Oakton, Vernon Hills, IL. Serial number: 448117.
- [22] Keith J. Laidler. Chemical Kinetics. Harper & Row, New York, NY, 3 edition, 1987.
- [23] Harry R. Allcock; Frederick W. Lampe; James E. Mark. Contemporary Polymer Chemistry. Pearson Education (Prentice-Hall) Inc, Upper Saddle River, NJ, 3 edition, 2003.

Appendix A

A.1 Procedure for pH Calculation for Known Acid Solutions

For

$$K_a = \frac{[H^+][B^-]}{[HB]} \quad (\text{A.1})$$

and having all concentrations in molarity, we set:

$$x = [H^+] = [B^-] \quad (\text{A.2})$$

$$C = [HB]_0 \quad (\text{A.3})$$

For the systems used in this study, the total concentration is the summed concentration of acid in the aqueous phase and acid in the oil phase respectively, equation A.4. It is assumed that the concentration of acid species is equivalent for both aqueous and oil phases at 100 °C, represented by equation A.5.

$$C = [HB]_{aq} + [HB]_{oil} \quad (\text{A.4})$$

$$C = 2[HB]_{aq} \quad (\text{A.5})$$

Since the acid only deprotonates in the aqueous phase, we obtain equation A.6.

$$\frac{C}{2} = [HB]_{aq} \quad (\text{A.6})$$

And to calculate the concentration of protonated acid species at any given time, equation A.7.

$$[HB] = \frac{C}{2} - x \quad (\text{A.7})$$

and substitute into equation A.1 to get equation A.8.

$$K_a = \frac{x^2}{\frac{C}{2} - x} \quad (\text{A.8})$$

Setting x on one side we get equation A.9.

$$K_a\left(\frac{C}{2}\right) - K_ax - x^2 = 0 \quad (\text{A.9})$$

Solving for x and using the association displayed in equation A.10 the pH for each solution was obtained.

$$pH = -\log(x) \quad (\text{A.10})$$

To calculate the theoretical pH per given solution for the qualitative comparison presented the parameters listed in Table A.1 were used.

Linear Carbons	Acid Name	pKa	Ka	Density ($\frac{g}{mL}$)	Molar Mass ($\frac{g}{mole}$)	Volume (mL)
1	Acetic	4.75	$1.78e^{-5}$	1.049	60.05	10
2	Propionic	4.87	$1.35e^{-5}$	0.992	74.08	10
3	Butyric	4.81	$1.55e^{-5}$	0.958	88.11	10
4	Pentanoic	4.82	$1.51e^{-5}$	0.935	102.13	10

Tables A.1: Parameters used to calculate the pH, Appendix A